CODEN:LUTEDX/(TEIE-7277)/1-52/(2020)

Industrial Electrical Engineering and Automation

Modelling Industrial Symbiosis of Biogas Production and Industrial Wastewater Treatment Plants – Technical Report

C. Kazadi Mbamba, M. Arnell, A. Bergvatten, J. Ejlertsson, U. Jeppsson, F. Ometto, A. Karlsson

Division of Industrial Electrical Engineering and Automation
Faculty of Engineering, Lund University

RI.
SE

BUILDT ENVIRONMENT
SYSTEM TRANSITION AND
SERVICE INNOVATION

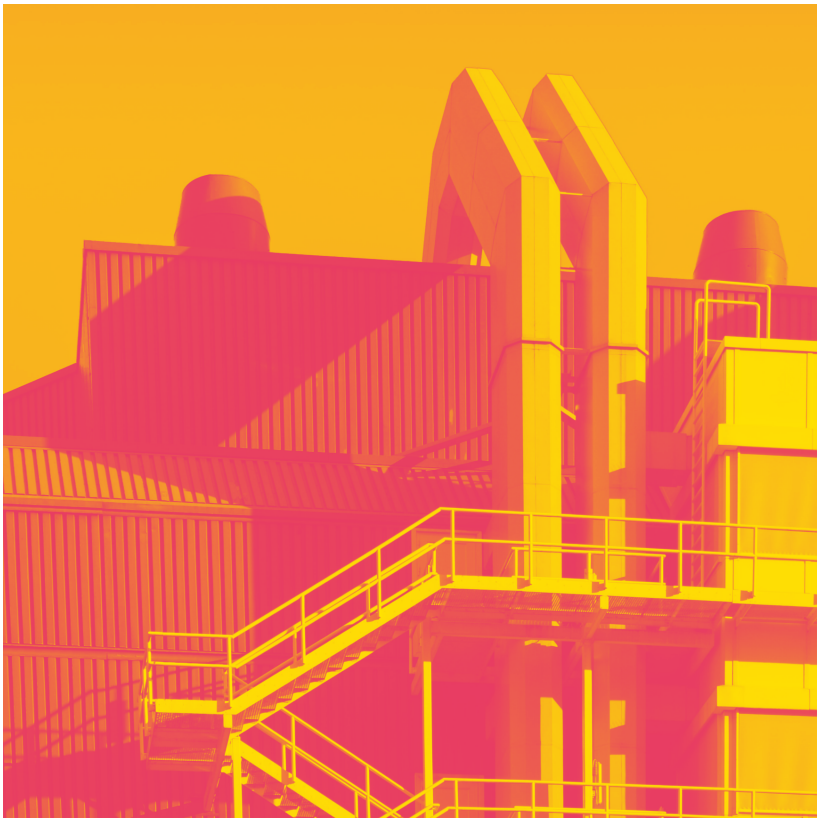

Modelling Industrial Symbiosis of Biogas Production and Industrial Wastewater Treatment Plants – Technical Report

Christian Kazadi Mbamba, Magnus Arnell,
Anders Bergvatten, Jörgen Ejlertsson, Ulf Jeppsson,
Francesco Ometto, Anna Karlsson

Modelling Industrial Symbiosis of Biogas Production and Industrial Wastewater Treatment Plants – Technical Report

Christian Kazadi Mbamba, Magnus Arnell, Anders Bergvatten, Jörgen Ejlertsson, Ulf Jeppsson, Francesco Ometto, Anna Karlsson

Abstract

Modelling Industrial Symbiosis of Biogas Production and Industrial Wastewater Treatment Plants – Technical Report

The present-day treatment of pulp and paper mill effluents can be significantly improved by incorporating biogas production in the context of industrial symbiosis. In this work a new industrial symbiosis concept is presented, the focus being on modelling it in view of process optimization, design improvement and adoption by the pulp and paper industry. The concept consists of a first stage in which pulp and paper mill effluents are treated by high-rate anaerobic digestion in external circulation sludge bed (ECSB) reactors to produce biogas. In the second stage the removal of organic matter contained in the anaerobic effluent stream occurs through aerobic activated sludge treatment, aiming to achieve maximum sludge production with minimum aeration requirements. This sludge should in the case study then be co-digested with residues from fish farming industry to yield methane for energy production, nutrient-rich reject water that can be recycled to the activated sludge treatment for optimum microbial activities and production of a nutrient-rich soil amendment. The overall research aim was in this project to develop a mathematical model that describes the relevant process units and the dynamics of the different processes involving organic matter removal, biogas production and nutrient release. The plant-wide model used integrated activated sludge and anaerobic models with a physico-chemical modelling framework. Through systematic calibration good general agreement was obtained between the full-scale experimental and simulated results at steady state. Acceptable differences between measured and modelled biogas production (flow rate and methane concentration), nutrients release (N and P) and effluent quality (N, P and COD) of 2-3.2 %, 5.3-7.4 % and 1.4-1.9 %, respectively, were observed throughout the full-scale system. Model-based analysis shows that the model can predict and give insight on dynamic behaviours resulting from deliberate changes but also on disturbances in one of the systems and their subsequent impacts within the integrated plant. Additionally, the model allowed the prediction of nutrients release in anaerobic digestion and subsequent consumption upstream in the high-rate anaerobic system or activated sludge system. Simulations show that there is a need for imposing a basic control and operational strategy for efficient reject water recirculation to optimize the concentrations of N and P in the activated sludge system while also achieving nutrient levels required to meet the effluent discharge permits. Overall, the evaluated plant-wide model can jointly describe the relevant physico-chemical and biological processes and is therefore advocated as a tool for future extension of this type of industrial symbiosis concepts between biogas producers and industries producing large amounts of wastewater rich in organic material. The model can be used for design, multi-criteria performance assessment and optimization of different treatment plants.

Keywords: Biogas, pulp and paper industry, wastewater treatment, industrial symbiosis, granular sludge bed reactors, anaerobic digestion, mathematical modelling

Acknowledgement: The authors acknowledge the financial support for the project by The Swedish Innovation Agency – Vinnova, (Dnr. 2017-03205).

Cover Illustration: Artwork – Magnus Arnell, Photo – Victor Garcia, unsplash.com

RISE Research Institutes of Sweden AB

RISE Report 2020:53
ISBN: 978-91-89167-36-0
Linköping, Sweden 2020

Table of contents

Nomenclature

AA	Amino-acids	
AcoD	Co-digestion	
AD	Anaerobic digestion	
ADM1	Anaerobic Digestion Model No. 1	
AnMBRs	Anaerobic membrane bioreactors	
ASM	Activated sludge model	
ASM2d	Activated Sludge Model No. 2d	
ASS	Activated sludge system	
BOD_7	7-day biochemical oxygen demand	($gO_2.m^{-3}$)
BSM2	Benchmark Simulation Model No. 2	
$CaCO_3$	Calcium carbonate	
CAS	Conventional activated sludge	
CH_4	Methane	(v/v%) or (g. m^{-3})
CI	Confidence interval	
CO_2	Carbon dioxide	(v/v%) or (g. m^{-3})
COD	Chemical oxygen demand	($gCOD.m^{-3}$)
CSTR	Continuous stirred-tank reactor	
CTMP	Chemi-Thermomechanical pulp	
DO	Dissolved oxygen	($g.m^{-3}$)
ECSB	External circulation sludge bed	
EGSB	Expanded granular sludge blanket	
H_2S	Hydrogen sulphide	(v/v%), (g. m^{-3}) (mole. L^{-1})
HRAS	High-rate activated sludge process	
HRT	Hydraulic retention time	(d)
IC	Internal circulation	
LCFA	Long-chain fatty acids	(g. m^{-3}) or ($gCOD. m^{-3}$)
MLSS	Mixed liquor suspended solids	($gSS.m^{-3}$)
MS	Monosaccharides	($gCOD. m^{-3}$)
N	Nitrogen	
NSSC	Neutral sulphite semi-chemical	
O_2	Oxygen	
OLR	Organic loading rate	($kgVS.m^{-3}d$)
P	Phosphorus	($gP. m^{-3}$)
pH	Hydrogen potential	(standard)
PO_4-P	Orthophosphate phosphorus	($gP.m^{-3}$)
PPI	Pulp and paper industry	
PPME	Pulp and paper mill effluent	
PS	Primary sludge	
RAS	Returned activated sludge	
SOO	Sulphur-oxidizing organisms	($gCOD. m^{-3}$)
SRB	Sulphate reducing bacteria	($gCOD. m^{-3}$)
SRT	Solid retention time	(d)
TIC	Total inorganic carbon	($gC.m^{-3}$)
TMP	Thermomechanical pulp	
TS	Total sulphur	($gS.m^{-3}$)
TSS	Total suspended solids	($gSS.m^{-3}$)
UASB	Upflow anaerobic sludge blanket	
VFA	Volatile fatty acids	($gCOD.m^{-3}$)
VS	Volatile solids	(w/w% of TS) or ($gVS.m^{-3}$)
VSS	Volatile suspended solids	($gVSS.m^{-3}$)
WAS	Waste activated sludge	
WWTP	Wastewater treatment pant	

Preface

This report is the final deliverable from the research project Modelling Industrial Symbiosis of Biogas Production and Industrial Wastewater Treatment Plants, running from 2017 to 2020. The project is funded by Sweden's Innovation Agency Vinnova and the leading project partner Scandinavian Biogas Fuels AB. Key partners of the project are Scandinavian Biogas Fuels AB, RISE Research Institutes of Sweden and Lund University (Division of Industrial Electrical Engineering and Automation).

Circular economy is a recent term to express the need for low emission, resource efficient and recycling processes for societies and industries. Industrial symbiosis is a means for achieving circular economy through interconnection of production facilities where one industry benefits from the resources (sometimes considered as waste) from another and then forward (or feedback) resources to a third user. The highly resource intensive pulp and paper industry (PPI) is one interesting sector for industrial symbiosis. One option to obtain a better energy balance for pulp and paper production and other industries generating organic wastes/ residues, is to use this material as substrates for biogas production. The world´s biogas production can be increased and geographically spread by exploring this today largely unused potential, thus contributing to climate change commitments worldwide. If these wastes or residues are co-digested with other more nutrient rich material a feedback of nutrients needed in the wastewater treatment of the PPI can also be achieved. These measures will both reduce costs and contribute to climate change mitigation. Furthermore, the biosolids can be used as fertilizer by nearby farms.

Within the project a modelling tool, able to assess the interactions of this circular economy concept has been developed. In this report the symbiosis concept is described through a specific case study (Chapter 1). Extensive modelling work including data collection and reconciliation was conducted to provide a calibrated and validated model to predict plant performance (Chapter 2 and 3). The plant-wide impact of integrating the two processes were assessed in a series of simulation scenarios investigating both benefits of the concept, optimization opportunities and potential risks (Chapter 3 and 4). Conclusions and ideas of future research is also presented (Chapter 5 and 6).

Christian Kazadi Mbamba, RISE,
Magnus Arnell, RISE,
Anders Bergvatten, Scandinavian Biogas Fuels,
Jörgen Ejlertsson, Scandinavian Biogas Fuels,
Ulf Jeppsson, Lunds universitet,
Francesco Ometto, Scandinavian Biogas Fuels,
Anna Karlsson, Scandinavian Biogas Fuels

Linköping, June 2020

1 Introduction

1.1 Background

The pulp and paper industry (PPI) is a large consumer of water (e.g. debarking, pulp preparation, bleaching water and boiler feed water as well as cooling water system) and generates large quantities of wastewater effluents that contain significant amounts of biodegradable and non-biodegradable organic material. Typical treatment approaches for pulp and paper mill effluents (PPME) involve a sedimentation step to remove suspended solids, and a biological treatment process, usually an activated sludge system (ASS), whereby organic matters are oxidized by the introduction of oxygen (air) into the wastewater (Pokhrel and Viraraghavan, 2004). ASS requires a large amount of energy for aeration to support the oxidation of organic matter (COD) and is often run at a high solid retention time (SRT), which results in a low waste activated sludge (WAS) production (Eddy et al., 2013). The high organic load and long retention times also mean that large basin volumes are needed for mineralization of organics in the ASS. Furthermore, unlike municipal wastewater, effluents from pulp and paper plants are deficient in vital nutrients like nitrogen (N) and phosphorus (P) that must be added to guarantee an efficient biological wastewater treatment (WWT) (Meyer and Edwards, 2014). The WAS produced in the ASS is typically considered waste and as such handled by incineration, which is becoming restricted due to emissions of greenhouse gases (Veluchamy and Kalamdhad, 2017). Hence, the current operation of wastewater treatment in PPI results in a loss of resource (i.e. energy and nutrients) recovery potential.

On the other hand, industrial symbiosis offers a pathway for achieving circular economy when interconnected industrial entities exchange resources (by-products) leading to waste reduction and decreasing adverse environmental impacts. Closing material loops while turning waste streams into useful and valuable input to other production processes or products have been the target of urban water management and is an essential element for sustainable industrial waste and water management. In this respect, an innovative industrial symbiosis concept aimed at increasing profitability and competitiveness of primary industrial partners, namely pulp and paper- and biogas producers, has recently been proposed and demonstrated (Magnusson et al., 2018). The benefits of such a partnership include higher production of non-fossil fuel (biomethane), reduction of the cost of resources needed (i.e. nutrients), reduction of energy use and substantial environmental improvements. Briefly, as shown in Figure 1 the concept includes high-rate anaerobic digestion of pulp and paper mill effluents designed to produce biogas. The anaerobic effluent stream is then further treated in an aerobic activated sludge process with a twofold purpose: to further reduce the organic matter content and to achieve maximum sludge production thus producing a digestible biosludge while keeping the aeration requirements to a minimum. To augment the potential of biogas production and profitability of the biogas plant, the WAS stream needs to be co-digested with other more energy and nutrient rich substrates, in continuous stirred tank reactors (CSTR). The digestate produced can then be refined by dewatering thus producing a solid cake, which can be used as bio-fertilizer/soil-improver, and a liquid stream rich in nitrogen and phosphorus that can be concentrated by evaporation. In case the biogas plant is co-located with a wastewater treatment plant treating wastewater with low nutrient content, the liquid digestate phase can be recirculated to the ASS thus reducing the need of external N and P (Meyer and Edwards 2014). This concept demonstrates an excellent industrial

symbiosis case where all the involved parties benefit from the synergy through substantial energy savings, low costs for sludge handling, no need for untreated digestate transportation over long distances and reduced use of commercial nutrients.

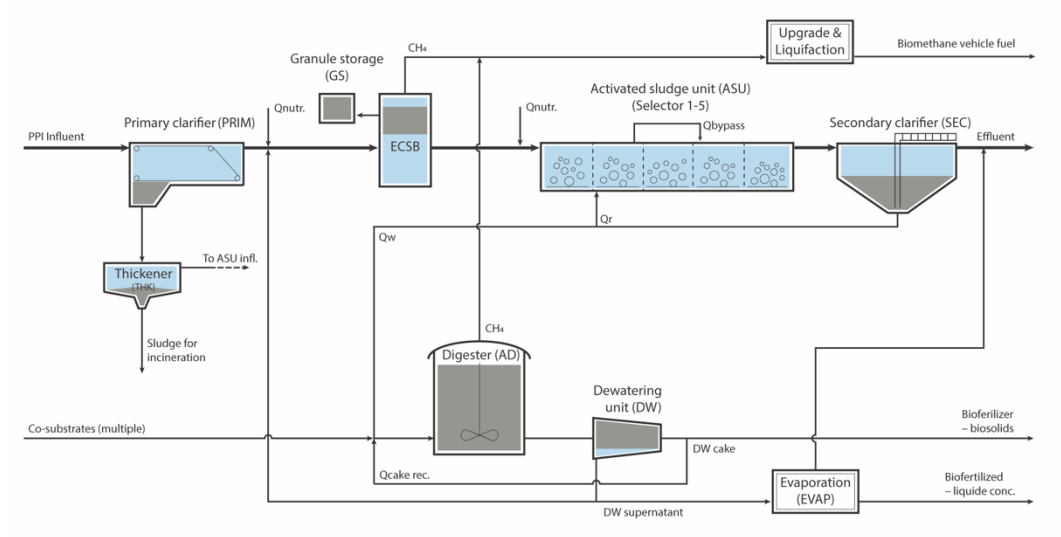

Figure 1. Simplified schematic overview of the industrial symbiosis between the biogas plant and the pulp and paper mill effluent treatment plant.

1.2 Modelling opportunities

The above circular economy concept is of great interest to PPI as it gives an opportunity to enhance sustainability, increase productivity and cost-competitiveness owing to large potential savings in energy and commercial nutrient consumption (Stoica et al., 2009). However, the lack of a general model may hamper the efforts aimed at accelerating knowledge transfer and diffusion of technology to as many mills and wastewater treatment plants as possible.

In this respect, there is a need for the development and application of improved integrated industrial symbiosis modelling tools for the assessment of biogas processes in synergy with pulp and paper mill effluent treatment. A comprehensive mathematical model is a valuable tool for gaining insight into the dynamics of the systems due to variations in operational conditions in the involved processes. Other benefits of modelling an industrial symbiosis are improvements in design, assessment of process configuration, evaluation of operational and control strategies technology development and model-based optimization and design. Process models can also be used as an evaluation and decision support tool purposed to deliver cost savings in operational expenditure.

Various industry-standard models have been developed to assess and simulate the performance of wastewater treatment. These models include the popular IWA activated sludge model (ASM) series for activated sludge systems (Gernaey et al., 2004; Henze, 2000) and IWA anaerobic digestion model no1 (ADM1) developed for describing biogas production (Batstone et al., 2002). While the ASM series were primarily developed for evaluating municipal wastewater treatment performance, few studies have used them to simulate activated sludge system treating pulp and paper mill effluents with satisfactory outcomes for the required purposes (Brault et al., 2010; Horan and Chen, 1998). On the other hand, ADM1 has been applied for biogas production and COD reduction from pulp and paper mill effluent. To date,

no integrated model exists for an industrial symbiosis centred on biogas production (anaerobic digestion and co-digestion) for pulp and paper effluents and some of the processes included in the industrial symbiosis described above are not fully compatible with traditional state-of-the-art process models. This is because the evaluation criteria of conventional treatment technologies are currently focused on quality of treated wastewater, whereas model requirements are considerably more complex when the focus is biogas production and resource recovery technologies (Batstone et al., 2015). The contaminants present in pulp and paper wastewater may also differ from those present in municipal wastewater. This poses significant technical risks, because current models cannot estimate treatment plant performance once emerging technologies have been integrated, and a designed facility may not achieve legislated environmental performance requirements. Modelling pulp and paper mill wastewater treatment and biogas plants driven mainly by resource recovery technologies is an essential development that requires a holistic approach, providing integrated and flexible software tools to transition linear treatment systems into circular biogas resource recovery systems.

1.3 Project objective

To address the above-stated challenges and new opportunities**,** the main objective of this study is to select/develop and calibrate a comprehensive mathematical process model for systematic evaluation of the proposed industrial symbiosis concept as well as carry out sustainability assessments through steady state and dynamic simulations. The mathematical plant-wide model should describe the relevant process units, the interaction and the dynamics of the different processes involving organic matter removal and biogas production as well as nutrient release/recirculation. While the underlying principles of modelling individual units have already been established, the focus in this study centres on selecting the simplest, most robust and easily extendable integrated model that can predict the performance of the industrial symbiosis carrying out biological nutrient removal, biogas production and macronutrient recycle. This will advance the development and application of simulation techniques in biogas processes as well as support and encourage the transition of pulp and paper wastewater treatment towards a higher resource efficiency. The developed model can provide good insights in new projects to show the potentials for saving both electricity and nutrient additions in the WWT and predict discharge values for organic matter (COD), suspended solids (TSS), nutrients (such as N and P) etc. To demonstrate the robustness of the concept, the model can also be used to perform different scenario analyses under conditions that may cause process disturbances/failure.

2 Methodology

2.1 Description of industrial symbiosis

The integrated model of the industrial symbiosis was applied on a specific case, a full-scale set-up in connection to a Nordic pulp and paper mill. The mill treats roughly 900,000 tonnes per year of timber/wood chips by thermomechanical pulping (TMP) generating 500,000 tons of paper and from this production about 15 m^3 process water per ton of paper produced.

The pulp and paper effluent treatment plant at the mill treats an average of 21 000 $m^3.d^{-1}$ of wastewater. The original treatment plant was a fully aerobic activated sludge plant consisting of primary sedimentation, aeration reactors and secondary sedimentation. This treatment plant has now been integrated within an industrial symbiosis system which, in addition to the original treatment plant, consists of an external circulation sludge blanket (ECSB) plant and a CSTR plant for biogas production from various substrates (Figure 1).

2.1.1 ECSB plant

Prior to the ECSB plant, the process water from the paper mill is treated in a primary clarifier to remove easily settleable solids. The water then enters the ECSB plant, which consists of two identical units operating in parallel. Each unit is comprised of one neutralization tank (NT) and one ECSB reactor tank, connected as shown on the schematic overview in Figure 2. The NTs have a volume of approximately 250 m^3 each and the ECSB reactors have a volume of approximately 2 000 m^3 each. The incoming wastewater stream is split between the two parallel units and enters the NTs where it is mixed with recycled effluent from the ECSB reactors. NaOH, urea solution and phosphoric acid, required for optimal bacterial activities, can be added to the inlet of the NTs if needed. The water from the NT is pumped to the bottom of the ECSB reactor where it passes through the sludge blanket. In the sludge blanket, biogas is produced through anaerobic degradation of the soluble organic matter in the wastewater. The expansion of the sludge blanket is created by the upward flow of water from the NT and the produced biogas. Part of the effluent from the ECSB reactor is recycled to the NT to maintain a constant flowrate through the system. In addition, through the recycling of the ECSB effluent, alkalinity is recovered, thus reducing the addition of NaOH required for pH control. The part of the effluent which is not recycled leaves the system by means of the effluent discharge piping. It should be noted that this kind of high rate upflow AD-process which is dependent on a sludge bed with good settling properties is sensitive to suspended solid and the incoming wastewater should therefore ideally not contain suspended solids concentrations above 500-1 000 mg/l.

Although the ECSB plant during the time of the study had only one operational ECSB unit, which was used as part of the model calibration process, the design concept incorporating two parallel ECSBs was simulated for integrated model performance assessments.

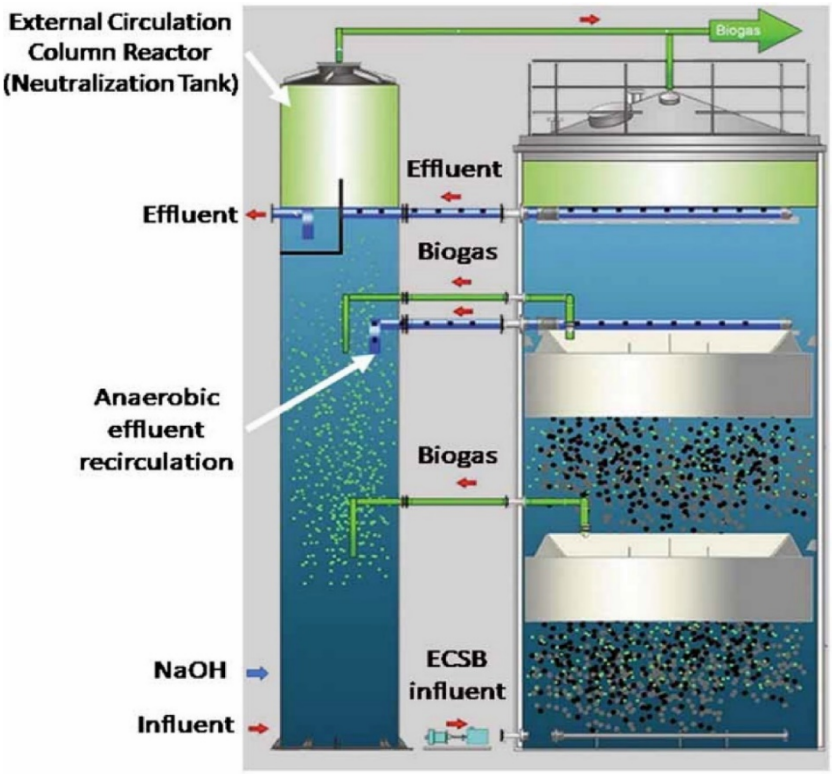

Figure 2. Schematic representation of an external circulation sludge bed (ECSB) reactor and neutralization tank (Diamantis and Aivasidis, 2018).

2.1.2 Activated sludge treatment plant

After treatment in the ECSB system the wastewater still contains a high concentration of organic materials that are further biodegraded under aerated conditions in the activated sludge system (ASS), which is a fully aerobic activated sludge plant consisting of aeration and secondary sedimentation. The plug-flow bioreactor system is a circular tank divided into five different zones (denoted selectors). The sizes are 1 500 m^3, 4 000 m^3, 10 300 m^3, 7 080 m^3 and 10 300 m^3 for selector 1, selector 2, selector 3, selector 4 and selector 5, respectively. The total volume of the aeration basin is 33 180 m^3. The aeration is regulated to give an oxygen concentration in the wastewater of around 2 mg/L. Activated sludge from the bioreactors is settled in a secondary clarifier. The effluent of the secondary clarifier is discharged to the sea whereas the returned activated sludge (RAS) is returned to the ASS. A volume of waste activated sludge (WAS) is removed from the base of the settler to maintain a specific sludge age. Nitrogen and phosphorus additions are needed to support the growth of the flora in the ASS, and are typically dosed as urea and phosphoric acid, respectively, to the influent entering the activated sludge system. However, the nutrients coming with the reject water from the completely stirred tank reactors (CSTRs; see below) means a decreased demand for external N and P.

2.1.3 CSTR plant

The anaerobic CSTR digestion plant, is designed for treating substrates such as fish (salmon) silage, seed fish sludge, slaughter house waste etc. together with excess biosludge (WAS) from the ASS treatment plant. The process was at the time of sampling treating salmon silage, seed fish sludge, cow manure and WAS. The CSTR plant has two parallel anaerobic digesters, each with an active volume of 6 560 m^3. Primary effluent is also fed to the digesters together with a

blend of dewatered and untreated digestate that is recirculated in the system. Digested substrates are discharged by gravity from the digesters to the digested sludge storage tank, then pumped to the sludge dewatering station. The reject water (centrate) from the dewatering, containing high concentrations of ammonia nitrogen and phosphate, is pumped to a reject buffer tank, from where a portion is recycled to before the ECSB-plant.

2.2 Wastewater characterisation

2.2.1 Design and process data

Daily average data were obtained from the extensive database collected by the operators of each system involved in the industrial symbiosis. Data acquisition included design data, flow rates of biogas, water and sludge streams and air to the activated sludge system.

2.2.2 Routine measurement data

The compositional analysis was measured and recorded as part of routine offline plant monitoring. These data included routine weekly or biweekly measurements on composite samples from the influent, primary effluent, effluent (treated outflow), bioreactors, return sludge and waste sludge, anaerobic digesters, and centrate (reject water). Analyses on the influent and effluent included chemical oxygen demand (COD), 5-day biochemical oxygen demand (BOD_5), total solids (TS), volatile solids (VS), total suspended solids (TSS), volatile fatty acids (VFA, acetic, propionic, iso-butyric and valeric acid), ammonia (NH_4-N), nitrate (NO_3^-), total Kjeldahl nitrogen (TKN), phosphate (PO_4-P), total phosphorus, alkalinity, soluble calcium (Ca), magnesium (Mg), sodium (Na) and potassium (K). Analyses were generally done using Standard Methods (APHA 2012). MLSS was measured and the solid retention time (SRT) or sludge age was controlled by manipulating the WAS flowrate in the activated sludge plant. The SRT was calculated as follows:

$$SRT = \frac{VX}{(Q - Q_w)X_e - Q_w X_R} \quad (1)$$

where V, X, X_e are the volume of the bioreactor, the MLSS and the suspended solids in the effluent, respectively. Q and Q_w are the flowrate in the activated sludge system and the effluent flowrate, respectively.

Data collected from 7/05/2019 to 15/05/2019 were used for the influent characterisation, whereas data collated over the period from 27 July 2019 to 7 August 2019 were arbitrarily selected and averaged before use as a representative measure of steady state conditions.

2.2.3 Intensive sampling and offline analysis

Intensive grab sampling and offline analyses were carried out to augment routine measurements at the plant. Grab samples were collected over two periods 7-15/05/2019 and 27/7-7/8/2019 from the influent, primary effluent, mixed liquor, and anaerobic digestate sludge from the recirculation pumps of the anaerobic digesters. The samples were centrifuged and filtered using 0.45 μm (Millipore, USA) and stored at 4 °C until further analysis. Sample vials were then stored in a cooler box with ice bricks and transported to external analytical laboratories. As indicated above, all the samples were characterized for soluble composition using Standard Methods (APHA, 2012).

2.3 System-wide model

2.3.1 Introduction

The implementation of a model to describe the industrial symbiosis required an integrated model platform including models such as activated sludge models and anaerobic digestion models (ADM1), which have not been developed in a plant-wide context and, importantly, do not have a common state variable set. In general, two main approaches have been used to develop plant-wide models. In the first approach individual models are linked via model interfaces that convert the states of one model into the corresponding states of another model (Jeppsson et al., 2007; Nopens et al., 2009). This approach is relatively flexible, allows connection of existing standard models (ASM and ADM1), and reduces computational redundancies. The BSM2 uses such interfaces (Gernaey et al., 2004). An alternative to the interfacing approach is applying a comprehensive model or a "supermodel" to describe all the state variables and process expressions across an entire wastewater treatment plant (Barat et al., 2013; Seco et al., 2004). The main advantage with the supermodel is that it avoids losing information when mapping one model's output to another model's input. Thus, the supermodels are mostly used in the commercial software of the wastewater industry. However, the supermodel approach is less flexible than the alternative (interfaces) and is not easily expanded or contracted when new state variables or components need to be added or removed. This plant-wide study used SUMO, a commercial software which architecture is based on the supermodel approach with a consistent set of state variables, stoichiometry and process rate equations, maintained throughout the integrated model (SUMO 19.2.0, Dynamita, Nyons, France, 2019).

2.3.2 Plant configuration

The integrated model of the industrial symbiosis includes pH and minerals precipitation models as well as a combined activated sludge and two-population anaerobic digestion model. The system-wide model configuration includes an interconnected ECSB plant, ASS plant and CSTR models. The existing process flow diagram of the plant under study was applied to build the plant-wide model configuration making use of graphical library blocks from the SUMO simulator described elsewhere (Hauduc et al., 2018; Varga et al., 2018). Briefly, the primary settling tanks were modelled as one non-reactive settler. Biochemical kinetics were described by a comprehensive model that has the same set of state variables for both the activated sludge and the anaerobic digestion systems, expanded to include physicochemical processes. The behaviour within the high-rate anaerobic digester (i.e. external circulation sludge blanket (ECSB)) was modelled using a CSTR system followed by an ideal suspended solids separator, known from previous studies as apparent kinetics approach (Baeten et al., 2019). For model simplicity, the ECSB system was modelled as a single line, without considering two units in parallel (lumped approach). The secondary settling tank was modelled as one non-reactive settler with some of the settled biomass collected midpoint of the settler to be recycled back to the activated sludge as returned activated sludge while the waste activated sludge left from the base of the settler to control the sludge age. For simplicity and simulation efficiency, the two parallel anaerobic digesters were also modelled as one volume.

2.3.3 Biochemical-chemical model

The development of the industrial symbiosis model has been divided into three major sections. The first section describes the overall activated sludge model. The second focuses on modelling anaerobic digestion processes including modelling the external circulation sludge bed (ECSB). Finally, the physico-chemical processes are described to depict the pH and precipitation model. The simulator SUMO uses a general super-model consisting of a combined model of activated sludge and anaerobic digestion, which is referred to as SUMO2S. The Gujer matrix describing the modelled processes in detail is available online (http://www.dynamita.com/the-sumo/).

2.3.4 Model state variables

To accurately model the different processes of the industrial symbiosis, a wide range of single models describing unit processes must be integrated through the water and sludge lines. The key features of the symbiosis model include carbon removal, nutrients, biogas production and sulphur conversion within the integrated activated and anaerobic digestion processes. SUMO2S has more than fifty state variables and over seventy kinetic processes. To model nutrient-deficient wastewaters from pulp and paper mills, variables and processes such as denitrification and biological phosphorus removal were omitted; however, limitations resulting from nitrogen and phosphorus deficient conditions on ordinary heterotrophic organism growth were included in the activated sludge and anaerobic digestion models. Table 1 presents the model state variables for soluble and particulate components included in the model.

Table 1. Relevant variables included in the integrated model. Full list of state variables in SUMO2s is available in SUMO documentation.

Symbol	Symbol	Unit
Volatile fatty acids	S_{VFA}	g COD.m^{-3}
Readily biodegradable substrate	S_B	g COD.m^{-3}
Colloidal biodegradable substrate	C_B	g COD.m^{-3}
Slowly biodegradable substrate	X_B	g COD.m^{-3}
Soluble unbiodegradable organics	S_U	g COD.m^{-3}
Colloidal unbiodegradable organics	C_U	g COD.m^{-3}
Particulate unbiodegradable organics	X_U	g COD.m^{-3}
Endogenous decay products	X_E	g COD.m^{-3}
Anaerobic endogenous decay products	$X_{E,ana}$	g COD.m^{-3}
Ordinary heterotrophic organisms	X_{OHO}	g COD.m^{-3}
Aerobic ammonia oxidizers	X_{AOB}	g COD.m^{-3}
Nitrite oxidizers	X_{NOB}	g COD.m^{-3}
Acidoclastic methanogens	X_{AMETO}	g COD.m^{-3}
Hydrogenotrophic methanogens	X_{HMETO}	g COD.m^{-3}
Acidoclastic sulphate-reducing organisms	X_{ASRO}	g COD.m^{-3}
Hydrogenotrophic sulphate-reducing organisms	X_{HSRO}	g COD.m^{-3}
Sulphur-oxidizing organisms (S_{OO})	X_{SOO}	g COD.m^{-3}
Total ammonia (NH_x)	S_{NHx}	g N.m^{-3}
Nitrite (NO_2)	S_{NO2}	g N.m^{-3}
Nitrate (NO_3)	S_{NO3}	g N.m^{-3}

Dissolved nitrogen (N_2)	S_{N2}	g N.m^{-3}
Soluble biodegradable organic N (from S_B)	$S_{N,B}$	g N.m^{-3}
Particulate biodegradable organic N (from X_B)	$X_{N,B}$	g N.m^{-3}
Particulate unbiodegradable organic N	$X_{N,U}$	g N.m^{-3}
Orthophosphate (PO_4)	S_{PO4}	g P.m^{-3}
Soluble biodegradable organic P (from S_B)	$S_{P,B}$	g P.m^{-3}
Particulate biodegradable organic P (from X_B)	$X_{P,B}$	g P.m^{-3}
Particulate unbiodegradable organic P	$X_{P,U}$	g P.m^{-3}
Dissolved methane (CH_4)	S_{CH4}	g COD.m^{-3}
Dissolved hydrogen (H_2)	S_{H2}	g COD.m^{-3}
Total inorganic carbon (CO_2)	S_{CO2}	g TIC.m^{-3}
Inorganics in influent and biomass	X_{INORG}	g TSS.m^{-3}
Other strong cations (as Na^+)	S_{CAT}	g Na.m^{-3}
Other strong anions (as Cl^-)	S_{AN}	g Cl.m^{-3}
Calcium	S_{Ca}	g Ca.m^{-3}
Magnesium	S_{Mg}	g Mg.m^{-3}
Potassium	S_K	g K.m^{-3}
Hydrogen sulphide (H_2S)	S_{H2S}	g S.m^{-3}
Sulphate (SO_4)	S_{SO4}	g S.m^{-3}
Particulate elemental sulphur (S)	X_S	g S.m^{-3}
Ferrous ion (Fe^{2+})	S_{Fe2}	g Fe.m^{-3}
Active hydrous ferric oxide, high surface (HFO,H)	$X_{HFO,H}$	g Fe.m^{-3}
Active hydrous ferric oxide, low surface (HFO,L)	$X_{HFO,L}$	g Fe.m^{-3}
Aged unused hydrous ferric oxide (HFO,old)	$X_{HFO,old}$	g Fe.m^{-3}
P-bound hydrous ferric oxide, high surface (HFO,H,P)	$X_{HFO,H,P}$	g Fe.m^{-3}
P-bound hydrous ferric oxide, low surface (HFO,L,P)	$X_{HFO,L,P}$	g Fe.m^{-3}
Aged used hydrous ferric oxide, high surface (HFO,H,P,old)	$X_{HFO,H,P,old}$	g Fe.m^{-3}
Aged used hydrous ferric oxide, low surface (HFO,L,P,old)	$X_{HFO,L,P,old}$	g Fe.m^{-3}
Calcium carbonate ($CaCO_3$)	X_{CaCO3}	g TSS.m^{-3}
Amorphous calcium phosphate (ACP)	X_{ACP}	g TSS.m^{-3}
Struvite (STR)	X_{STR}	g TSS.m^{-3}
Iron sulfide (FeS)	X_{FeS}	g TSS.m^{-3}
Carbon dioxide gas (CO_2)	G_{CO2}	g TIC.m^{-3}
Methane gas (CH_4)	G_{CH4}	g COD.m^{-3}
Hydrogen gas (H_2)	G_{H2}	g COD.m^{-3}
Oxygen gas (O_2)	G_{O2}	g O.m^{-3}
Ammonia gas (NH_3)	G_{NH3}	g N.m^{-3}
Nitrogen gas (N_2)	G_{N2}	g N.m^{-3}
Hydrogen sulfide gas (H_2S)	G_{H2S}	g N.m^{-3}

2.3.4.1 Activated sludge processes

The processes included for organic carbon removal and nitrogen transformations are primarily based on those considered in the IWA ASM series and general dynamic model for nutrient removal systems (Barker and Dold, 1997; Henze, 2000). However, modifications

were carried out to suit the general characteristics of the pulp and paper mill effluents. Bio-P processes are not included in the model since pulp and paper mill effluents are deficient in phosphorus.

The different dynamic processes included in the activated sludge model are described below:

- *Growth (and decay) of ordinary heterotrophic organisms (OHO)*: The OHO play a key role in the mineralization of organic compounds, particularly for industrial wastewater containing a high level of organics. The growth and death of OHO are described with VFA and readily biodegradable organics (S_B) as substrates and oxygen, nitrate or nitrite as electron acceptor, with ammonia nitrogen, nitrite or nitrate serving as the source of nitrogen for cell synthesis purposes.
- *Hydrolysis and adsorption of slowly biodegradable organics*: Heterotrophic microorganisms are assumed to participate in the general model in the hydrolysis of slowly biodegradable particulate substrate resulting in production of readily biodegradable complex substrate, which are then mineralized by the ordinary heterotrophic organisms.
- *Hydrolysis and solubilization of biodegradable particulate organic nitrogen and phosphorus:* The hydrolysis of biodegradable particulate nitrogen and phosphorus is assumed to proceed at the same rate as that of the biodegradable particulate organics but is adjusted by the ratio of biodegradable particulate organic nitrogen and phosphorus to biodegradable particulate organics.
- *Ammonification of soluble organic nitrogen to ammonia:* The conversion of organic nitrogen to ammonia nitrogen is mediated by the active OHO. The rate is the product of the ammonification rate constant, the soluble organic nitrogen concentration and the ordinary heterotrophic concentration.
- *Two-step nitrification processes:* These processes are very limited in an ASS treating PPME due to nitrogen deficiency. The two-step nitrification process is modelled with the first step of ammonia oxidation to nitrite performed by ammonia-oxidizing bacteria (AOB) and the second step where nitrite-oxidizing bacteria (NOB) oxidize nitrite to nitrate.
- *Processes involving sulphur oxidizing organisms:* These processes describe the growth of sulphur oxidizing organisms on H_2S and/or on particulate elemental sulphur using either oxygen, nitrite or nitrate as electron acceptor, and their decay under anaerobic conditions.

2.3.4.2 Anaerobic digestion processes

Two approaches for modelling anaerobic digestion processes are normally used depending on whether an interface or supermodel is applied in the plant-wide context. In the first approach, the ADM1 is typically used, whereas the second approach focuses on anaerobic digestion using the same state variables as in the activated sludge model. The latter approach excludes some intermediary processes such as hydrolysis of carbohydrates, proteins and lipids which do not have corresponding variables in the activated sludge models. In this study, a simple model based on the second approach was implemented. This basic model is a two-population model of the anaerobic food chain consisting of heterotrophs and acidoclastic methanogens (AMETO) and hydrogenotrophic methanogens (HMETO). (Figure 3).

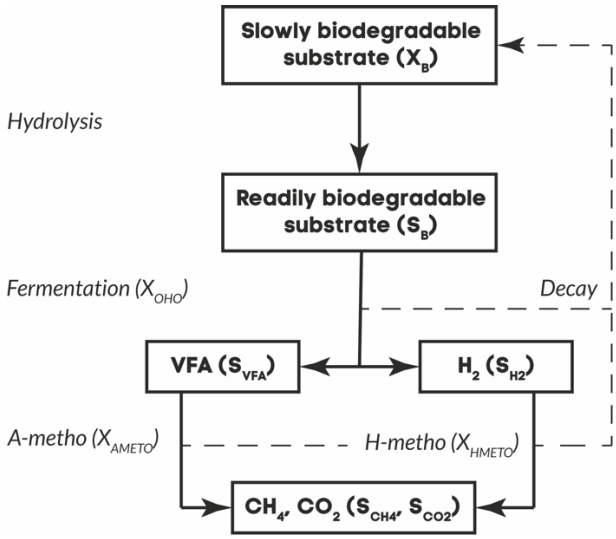

Figure 3. Simplified conceptual schematic for the anaerobic digestion model based on a two-population framework.

The main processes included in the integrated activated sludge and anaerobic digestion model are as follows:

- *Heterotrophic growth through fermentation*: The slowly biodegradable substrate fraction is first converted to readily biodegradable substrate, which is then fermented to VFA, carbon dioxide and hydrogen by ordinary heterotrophic organisms.
- *Processes of methanogens*: These processes describe the growth and decay of two of the principal groups of obligate anaerobic microorganisms: acetoclastic methanogens converting VFA to methane and CO_2, while hydrogenotrophic methanogens convert CO_2 and hydrogen to methane and water.
- *Processes of sulphate-reducing organisms*: These processes describe the oxidation of organic compounds for energy generation and cell growth using sulphur compounds as electron acceptors leading to the production of hydrogen sulphide. These bacteria are in direct competition with hydrogenotrophic and acetoclastic methanogens in anaerobic processes.

2.3.4.3 Physico-chemical model

A physico-chemical model is included in the integrated model to determine the aqueous speciation system including the pH and the concentrations of ions and undissociated components, as well as the precipitation and dissolution of minerals. The physico-chemical model is inextricably linked to the biological models through the state variables, and allows the pH, ions, and mineral state variables to be determined at any time from the total component concentrations in the system. The main model structure consists of two parts: equilibrium and precipitation/dissolution.

Speciation model (pH model)

The speciation or equilibrium part of the physico-chemical model encompasses an equilibrium equation set describing instantaneous phase reactions such as weak-acid and ion pairs. The implicit algebraic equation set of the equilibrium part consists of a reduced substituted

combination of equilibrium relationships, molar contribution balances and a charge balance equation. Due to high concentrations of divalent and trivalent ions in the digesters in this study, the equilibrium model needed to account for non-ideal conditions for all the relevant ion pairing and activity to enable accurate pH prediction. However, SUMO uses a simplistic approach for modelling the aqueous system with limited amount of ion pairs. In this respect, an improved physico-chemical framework (Kazadi Mbamba et al., 2015) with all the relevant ion pairs was implemented; however, the simulations were found to be several orders of magnitude slower because a fully kinetic approach was used for both fast reactions (e.g. acid-base systems) and slow reactions (e.g. minerals precipitation reactions). This approach works well but increases the number of dynamic state variables. A combined kinetic-equilibrium approach, allowing rapid processes to be treated with an algebraic equation set, while the slow kinetic processes are treated via a differential equation set, would be suitable but could not be implemented in the current version of SUMO. Due to computational issues, the implementtation of the improved physico-chemical model was not carried further. The existing physico-chemical model in SUMO was tested with a digestate system having an ionic strength of about 0.5 M and the pH predication was found to be within 10 % of accuracy of Visual Minteq, a geochemical physico-chemical model. Hence the simulations reported in this study were carried out with the existing pH model (corrections of activity coefficients and ion pairing) in SUMO.

Precipitation/dissolution model

The biological models, particularly the anaerobic digestion model, include chemical precipitation processes of minerals, namely calcite ($CaCO_3$), amorphous calcium phosphate ($Ca_3(PO_4)_2$), struvite ($MgNH_4PO_4$) and iron sulphide (FeS). Mineral precipitation is described as a reversible process using supersaturation as the chemical driving force. The rate expression for mineral precipitation (for example struvite) of the form proposed by Koutsoukos et al. (1980) was used:

$$r_{MgNH4PO4} = k_{MgNH4PO4} X_{MgNH4PO4} \sigma^n \quad (2)$$

where $r_{MgNH4PO4}$ is the struvite precipitation rate (gTSS.m^{-3}.d^{-1}), $k_{MgNH4PO4}$ is an empirical kinetic rate coefficient (d^{-1}), $X_{MgNH4PO4}$ (gTSS.m^{-3}) is the concentration of struvite precipitate at any time *t* (a dynamic state variable). *n* is the order of the precipitation reaction (equal to 3 for struvite) with respect to supersaturation, calculated as follows for iron phosphate as an example:

$$\sigma = \left(\frac{Z_{(Mg^{2+})} x \; Z_{(NH_4^+)} x \; Z_{(PO_4^{3-})}}{Ksp_{MgNH4PO4}} \right)^3 - 1 \quad (3)$$

where $Z_{(Mg2+)}$, $Z_{(NH4+)}$ and $Z_{(PO43-)}$ are the chemical activities of magnesium, ammonium and phosphate ions in the aqueous phase and $K_{SP,MgNH4PO4}$ is the solubility product constant for iron phosphate.

2.3.5 Influent characterization

2.3.5.1 Influent COD fractionation modelling

The success of plant-wide modelling projects largely depends on the characterization of the influent. This is particularly important for pulp and paper mill effluents, which comprise a complex mixture of organic and inorganic material as well as nutrients, which must be characterised in terms of the state variables of the model in use. The organic matter (total COD) in the influent was fractionated into volatile fatty acids (S_{VFA}), readily biodegradable substrate (S_B, soluble non-VFA), colloidal biodegradable substrate (C_B), inert soluble unbiodegradable organic compounds (S_U), slowly biodegradable organic compounds (X_B), colloidal unbiodegradable organics (C_U) and inert particulate unbiodegradable organics (X_U) as described by (Melcer, 2003). The fractionation of COD in the influent was performed using the routine data provided by the plant according to the standard guidelines for wastewater and sludge characterisation (Melcer, 2003). Briefly, the biodegradable COD ($S_{VFA} + S_B + C_B + X_B$) concentration was estimated based on BOD_5 test data. Soluble COD products (S_{VFA}) was estimated to be equal to measured VFAs. Readily biodegradable COD (S_{VFA}) was estimated using the flocculation-filtration procedure proposed by Mamais et al. (1993), based on the assumption that suspended solids and colloidal particulates are captured and removed by flocculation with a zinc hydroxide precipitate to leave only truly dissolved organic matter after filtration. The soluble colloidal fraction was determined as a difference between the measured soluble COD and the soluble flocculated COD ($C_B = sCOD - sfCOD$).

The soluble unbiodegradable COD concentration is obtained directly from the measured data. 90 % of the soluble COD measured in secondary effluent samples (treated outflow) is counted as unbiodegradable soluble COD (S_U). The unbiodegradable particulate organics (X_U) was determined after calibrating the primary effluent X_{TSS} and sludge age by matching the observed and predicted mixed liquor suspended solids concentration. The slowly biodegradable COD concentration was determined from previous process data and previously estimated influent fractions ($X_B = COD - S_{VFA} + S_B + C_B + S_U + C_U + X_U$).

In the model the wastewater macronutrients (N, P and S) also have different biodegradable and inert fractions which must be defined according to the model. For example, nitrogen is fractionated into ammonia N, soluble biodegradable organic N, colloidal biodegradable organic N, soluble unbiodegradable organic N, colloidal unbiodegradable organic N, particulate, unbiodegradable organic N and particulate biodegradable organic N. The same basis of fractionation is used for phosphorus and sulphur components.

The values of influent variables such as total suspended solids (X_{TSS}), total dissolved ammonia nitrogen (S_{NH4}), nitrate (S_{NO3}), inorganic soluble phosphorus (S_{PO4}), sulphate and sulphide were assumed to be equal to experimentally measured values (average measured from composite samples taken from the influent every three hours for three days). Other variables in the influent, such as gases and minerals (Table 1), were set to zero. Furthermore, particulate components, namely aerobic ammonia oxidizers (X_{AOB}) or nitrifying organisms (X_{NOB}), ordinary heterotrophic organisms (X_{OHO}), acidoclastic methanogens (X_{AMETO}), hydrogenotrophic methanogens (X_{HMETO}), acidoclastic sulphate-reducing organisms (X_{ASRO}), hydrogenotrophic sulphate-reducing organisms (X_{HSRO}) and sulphur-oxidizing organisms (X_{SOO}) were assumed undetectable in the influent.

2.3.5.2 Substrate characterization

The substrates (fish waste sludge, cow manure and seed fish sludge) used in the co-digestion unit together with the WAS were characterized using the methodology described above, except for the degradable COD fraction which was determined using results from batch biomethane potential (BMP) tests. All analyses were done at least in triplicate. The first-order hydrolysis coefficient and degradability of each substrate were estimated based on a simple first-order kinetic model (Jensen et al., 2011).

$$B_{(t)} = B_0 \times \left(1 - e^{-k_{hyd} \times t}\right) \quad (4)$$

where $B_{(t)}$ is the cumulative methane yield at time t (mL CH_4.gVS^{-1}), B_0 is the methane potential of the substrate (mL CH_4 .gVS^{-1}), k_{hyd} is the first-order hydrolysis rate constant and methane production rate constant (d^{-1}), which is determined by taking the reciprocal of the time from the start of the BMP test until the time when $B_{(t)}$ equals 0.632 B_0. The parameters B_0 and k_{hyd} were estimated by simultaneously fitting data from the BMP experiments using a non-linear parameter estimation technique in MATLAB or Excel. The methane yield was selected as the fitted output and the residual sum of squares (RSS) was selected as the objective function (J = RSS). The model was implemented in MATLAB. Errors in parameters were generally estimated by two-tailed t-tests based on linear estimates of standard error, but when necessary, true confidence intervals were estimated based on an F-test in J as follows:

$$J_{crit} = J_{opt}\left(1 - \frac{p}{n_{data} - p}\right) F_{0.95,p,n_{data}-p} \quad (5)$$

where J_{crit} is the 95 % confidence objective function (where $p = p_{95}$), p is the number of parameters (2), n_{data} is the number of data points, and $F_{0.95,p,n_{data}-p}$ is the cumulative F distribution value.

The biodegradable COD fraction (f_d) was determined as a ratio between the maximum biomethane potential (B_0) and the measured total COD as follows:

$$f_d = \frac{B_0}{350 \times COD} VS \quad (6)$$

where COD is the total COD (kg COD. m^{-3}) and VS is the volatile solids (kg. m^{-3}).

As per Arnell et al. (2016), the unbiodegradable particulate and soluble organics are estimated using the measured values for filtered COD or total COD and the estimated degradability as S_U = sCOD(1-f_d) and X_U = COD(1-f_d), respectively. The soluble state variables including VFA and readily biodegradable (non-VFA) organics were calculated from measurements as described in Section 2.3.5.1.

2.3.5.3 Time-varying influent data generation

Since routinely collected process data are rarely sampled at enough frequency to capture the plant dynamics, an influent generator may be suitable for generating high frequency data. However, a simplified influent generator was deemed necessary for the industrial wastewater in this study which did not appear to show any consistent daily/weekly or seasonal patterns. In this case a raw influent flow dataset from 6/06/2018 to 5/06/2019 was used, having an average, a min and a max of 21096, 3707 and 28835 m^3.d^{-1}, respectively. High frequency flow

rate was generated with 1-hour resolution and (random) noise to ensure that subsequent days do not have the same flow rate profile.

2.4 Integrated model calibration

A plant-wide model has an increased level of complexity due to the large number of parameters to calibrate. The parameters of the models are not universal as most applications would require adjusting the model parameters against the measured process data. The strategy in this study was to minimise the number of parameters, which were chosen for calibration using a stepwise calibration methodology in the integrated plants.

The ECSB plant for the treatment of pulp and paper mill effluent was designed for biogas production and biodegradable COD removal. Thus, the calibration of the ECSB model focused on adjusting key parameters, such as the heterotrophic yield coefficient (Y_H), fraction of biomass to calibrate biogas flow and methane concentration in the gas, and COD, TSS, N and P in the ECSB effluent.

Calibration of the ASS treating pulp and paper effluent applies a simple strategy focussed mainly on COD removal, since the biological nutrient removal and transformation occurs to a very limited extent. The main parameters including growth rate, yield coefficient (Y_{OHO}) of heterotrophs and influent unbiodegradable particulate organics were adjusted accordingly to calibrate the TSS in the mixed liquor, RAS and WAS, and TSS and COD in the effluent. Excess NH_4 from dosing and ammonification undergoes nitrification. Nitrate and ammonia nitrogen concentrations in the secondary effluent were calibrated by adjusting the kinetics of autotrophic bacteria.

2.5 Model scenarios

Scenario analyses were used to investigate the integrated performance of the model and the impact of simultaneous precipitation on phosphorus removal under steady-state and dynamic conditions. The criteria that were used to assess model performance were effluent quality in the water line including soluble ammonia nitrogen, nitrate and phosphate. The following four scenarios were selected for model evaluation:

i) Scenario 1 (Base case) – plant-wide model with the ECSBs at full capacity. ASS sludge age of 17 days and 90 % of the ASS internal flow bypassing selector 3. The flow rate of the wastewater primary effluent (out of the primarily clarifier) was set to 21 549 $m^3.d^{-1}$ and 90 % of this was passed through the ESCB. The COD concentration of the primary effluent is given in Table 2. This scenario analysis was based on the calibrated model, with three changes: the volume of the ECSB was doubled; 90 % of the flow was bypassed selector 3 in the ASS; and 90 % of the biosludge treated was co-digested for biogas production. No urea was dosed to the system while H_3PO_4 was added both to the ESCB (A) and to the ASS (B).

The reason for leading 10 % of the primary effluent directly to the ASS without passing the ECSB is to keep the activity in the ASS on a higher level then possible if all wastewater was treated in the ECSB before going to the ASS. For the same reason 10 % of the total flow coming into the ASS is lead to selector 3 although this selector is not needed when the ESCB is active.

The COD concentrations and loads of the substrates going into the CSTR was in the scenario set to: COD 583 000 g.m-^{3} at a flow of 127 m^{3}.d^{-1} for fish silage, COD 90 300 at a flow of 10.9 m^{3} for cow manure and COD 139 000 at a flow of 16.3 m^{3} for seed fish sludge.

ii) Scenario 2 is the same as Scenario 1, except for the sludge age which was decreased to 8 days by increasing the sludge wasting rate (i.e. WAS flow). This scenario attempts to decrease the residence time of the sludge (sludge age) by half in the ASS to investigate the impact on plant effluent and biodegradability of the WAS in terms of biomethane potential.

iii) Scenario 3 was set to optimize the nutrient addition to the ECSB and ASS. The base case (Scenario 1) and Scenario 2 were used to optimize the dosing of nutrients and corresponds to Scenario 3a and 3b respectively). N and P mass flows were manipulated towards a predefined concentration of nitrogen in the ECSB effluent by adjusting mainly the reject water flow rates. This scenario examined whether optimization of a nutrient controller would be essential to achieve low N and P effluent values while at the same time avoiding too low N and P concentrations in the ASS, which would be detrimental to its biological processes.

iv) Scenario 4 – 100 % bypass of the primary effluent over the ECSB for specified times: 0.5, 1, 3, 5 and 7 successive days for both scenarios 1 and 2 under dynamic conditions.

The different scenarios above were analysed based on 200 days of simulation with dynamic influent conditions. To ensure that the model had reached steady state before beginning the analysis, a simulation was run for at least 200 days with a static influent and results at the end of this simulation was reused as initial values for the dynamic simulations.

3 Results

3.1 Steady-state plant influent

Influent data from 2018 (dataset 1) were used to fractionate COD used in the steady-state model calibration. Some of the COD estimates ratios were also used to characterize the missing data including flocculation-filtered COD, BOD and VSS (dataset 2) used for model validation. Table 2 displays the measured total, filtered and flocculation-filtered COD, compounds of N and P as well as other cations and anions in the influent and primary effluent. The samples of the wastewater from the pulp and paper mill (influent to the wastewater treatment) had an average concentration of about 4 500 g m^{-3} of total COD. The organic matter in the wastewater contained a significant amount of soluble and flocculation-filtered COD (53 % and 34 %, respectively). However, the WWT-influent was deficient in nutrients, such as nitrogen and phosphorus. About 2.4 % of the influent TN (10.2 $gN.m^{-3}$) and 32.3 % of TP (1.9 $gP.m^{-3}$) were ammonia nitrogen and phosphate respectively.

Table 2. Average (±95 CI) steady-state influent compositions of the full-scale WWTP used for influent characterization and model calibration (Dataset 1 from 7/05/2018 to 15/05/2018), steady state model influent validation (Dataset 2 from 27/7/2019 to 7/8/2019), and primary steady state effluent (outgoing from the primary sedimentation) used for model calibration (7/05/2018 to 15/05/2018).

Parameter	Dataset 1	Dataset 2	Primary effluent
Total COD ($gCOD.m^{-3}$)	4 810±322	3 510±694	2 600±154
Soluble COD ($gCOD.m^{-3}$)	2 550±372	2 030±65	2 360±178
Flocculation-filtrated COD ($gCOD.m^{-3}$)	1 680±264	-	1 603±220
BOD ($gO_2.m^{-3}$)	893±171		910±372
TSS ($gSS.m^{-3}$)	1 850±493	1 150±293	199±33
VSS ($gVSS.m^{-3}$)	1 490±527		211±18
Total Alkalinity ($g\ CaCO_3.m^{-3}$)	369±320		247±73
VFA ($gCOD.m^{-3}$)	222±89	199±109	251±53
SO_4^{2-} ($gS.m^{-3}$)	126±22	100±28	272±84
S^{2-} ($gS.m^{-3}$)	0.07±0.03		2.8±2.2
TS ($gS.m^{-3}$)	159±33	116±28	150±27
NH_4-N ($gN.m^{-3}$)	0.24±0.16	0.6±0.88	0.10±0.06
NO_3-N ($gN.m^{-3}$)	0.05	5.07±0.46	
TKN ($gN.m^{-3}$)	10.2±0.98	6.9±2.23	7.65±0.98
PO_4-P ($gP.m^{-3}$)	0.61±0.2	0.53±0.24	0.44±0.13
TP ($gP.m^{-3}$)	1.89±0.3	1.22±0.15	1.51±0.2
Ca ($g.m^{-3}$)	179±36	107±63	122±11
Fe(II) ($g.m^{-3}$)	0.15±0.04		0.34±0.3
Fe(III) ($g.m^{-3}$)	0.08±0.04		
Fe ($g.m^{-3}$)	0.17±0.03	0.13±0.03	0.13±0.05
K ($g.m^{-3}$)	20±1.98	22.9±3.4	21.7±1.9
Mg ($g.m^{-3}$)	6.36±0.56	4.88±0.85	6.42±1.9
Na ($g.m^{-3}$)	228±31	223±36	240±33
Cl ($g.m^{-3}$)	23±4.6		70±40
TIC ($g.m^{-3}$)	273±240	116±28	62.2±25

The concentration of the readily biodegradable fraction as indicated by the flocculation-filtrated COD (1 680 $gCOD.m^{-3}$) was very high, which shows that the extent of anaerobic digestion in the ECSB would be high as well. This is normal for this type pf wastewater due to its origin.

As indicated above, Dataset 1 and Dataset 2 were used for plant-wide calibration and validation purposes, respectively. Table 3 show only the various COD fractions from Dataset 2 for the pulp and paper mill effluent. The volatile fatty acids and biodegradable substrate fractions accounted for 5.7 % and 26.5 %, of the total COD, respectively. The modelled influent contained 30 % inert particulates, which is higher compared to domestic wastewaters. For municipal raw wastewater values of 15 to 25 % have been reported (Henze, 2000; Henze et al., 2008; Gernaey et al., 2014).

Table 3. Average steady-state COD fractionation of the pulp and paper mill effluent used for influent steady state model validation.

Parameter	COD fraction ($gCOD.m^{-3}$)	COD ratio (%)
Volatile fatty acids (VFA)	199	5.68
Readily biodegradable substrate (non-VFA)	930	26.5
Colloidal biodegradable substrate	345	9.86
Slowly biodegradable substrate	429	12.3
Soluble unbiodegradable organics	204	5.82
Colloidal unbiodegradable organics	346	9.86
Particulate unbiodegradable organics	1 050	30

Nutrients such as nitrogen and phosphorus are essential for biological wastewater treatment and their fractionation in the influent is equally important to the characterization of COD from a modelling perspective. Table 4 shows the estimated conversion factors used to determine the organic N and P fractions in the influent. These factors included those for colloidal biodegradable substrate ($i_{N,CB}$ and $i_{P,CB}$), colloidal unbiodegradable organics ($i_{N,CU}$ and $i_{P,Cu}$) and soluble unbiodegradable organics ($i_{N,SU}$ and $i_{P,SU}$) and were adjusted accordingly to obtain the best fit for organic nitrogen and organic phosphorus in the influent. In general, the nitrogen and phosphorus fractions of soluble COD and slowly biodegradable organic substrate were assumed to be very low in this study, compared to those of typical domestic wastewaters (Henze, 2000).

Table 4. Nutrient fractions used to determine the organic N and P in the influent.

Model parameters	Symbol	Default value	After influent calibration
Nitrogen			
N content of colloidal substrate (gN. $gCOD^{-1}$)	$i_{N,CB}$	0.03	0.0025
N content of soluble inerts (gN. $gCOD^{-1}$)	$i_{N,SU}$	0.05	0.006
N content of colloidal inert organics (gN. $gCOD^{-1}$)	$i_{N,CU}$	0.01	0.006
Phosphorus			
P content of colloidal substrate (gP.$gCOD^{-1}$)	$i_{P,CB}$	0.005	0.0002
P content of soluble inerts (gP.$gCOD^{-1}$)	$i_{N,SU}$	0.002	0.001
P content of colloidal inert organics (gP.$gCOD^{-1}$)	$i_{N,CU}$	0.005	0.005

3.2 Substrate characterization

Table 5 presents a summary of the co-substrates used in the CSTR system. All the substrates can be described as high strength, i.e. with concentrations multiple times higher than the influent wastewater. The fish waste silage also contained high concentration of total nitrogen (20 100 $gN.m^{-3}$), indicating the extent of ammonia nitrogen that could be released as a result of anaerobic digestion. There is much higher variability in the measured data in comparison to the wastewater data in Section 3.1, which could be attributed to the characteristics of the substrates, measurement errors and grab sampling methodology. Sampling and analyses of fish waste silage and seed fish sludge was particularly challenging owing to floatable materials, such as oil and grease, which made the sample preparation very tedious and the measurement less reproducible.

Table 5. Average steady-state composition of the co-substrates used for anaerobic digestion.

Parameters	Fish silage	Fish seed sludge	Cow manure	Biosludge
Total COD ($gCOD.m^{-3}$)	58 3000 ±6606	139 000±39105	90 300±37973	41661±2489
Soluble COD ($gCOD.m^{-3}$)	22 000±72057	42 700±18933	43 900±27564	736±344
Flocculation-filtered COD ($gCOD.m^{-3}$)				512±171
TSS ($gSS.m^{-3}$)	184 000±14765	39 900±19679	25 000±4127	30 200±2731
VSS ($gCOD.m^{-3}$)	154 000±12585	22 000±10008	15 600±3494	29 100±1765
Total alkalinity (4.5) ($gCaCO_3.m^{-3}$)				1 640±65
VFA ($gCOD.m^{-3}$)	0.86±0.25	8.03± 5.8	4.26±1.11	0.12±0.06
SO_4^{2-} ($gS.m^{-3}$)	611±248	454±356	193±163	
S^{2-} ($gS.m^{-3}$)	0.14±0.09	0.22±0.12	2.33	
S ($gS.m^{-3}$)	1530±102	622±479	555	
NH_4-N ($gN.m^{-3}$)	26±17.6	0.62±0.45	1 880±969	
NO_3-N ($gN.m^{-3}$)				
TN ($gN.m^{-3}$)	20 100±459	5 570	3 950	
TKN ($gN.m^{-3}$)	11 100±2187	6 500±8820	3 720±549	29.7±14.3
PO_4-P ($gP.m^{-3}$)	2 950±373	966±757	275±352	
TP ($gP.m^{-3}$)	2 510±127	1 090±571	654±137	197±65
Ca ($g.m^{-3}$)				125±27
Fe ($g.m^{-3}$)	83±43.8	7.12	109±50.8	0.23±0.07
K ($g.m^{-3}$)	2 530±557	742	3 900±1538	49.0±12.20
Mg ($g.m^{-3}$)	539±167	949±751	276±109	7.64±0.27
Na ($g.m^{-3}$)	3 850±1309	8 040±2307	596±262	174±84.2
Cl ($g.m^{-3}$)	6 740±2519	9 520±6076	646±749	13.6±6.6
TIC ($gC.m^{-3}$)	6.83±4.09	6.23±5.98	815±108	150
TS ($gTS.m^{-3}$)	291 000±7275	85 400±27229	84 300±20253	30 000±25888
VS ($gVS.m^{-3}$)	272 000±5508	62 000±22106	68 900±21430	1 310±1145

One of the crucial steps in the characterization of the substrates was determining the extent of anaerobic biodegradability. Table 6 and Figure 4 present a summary of the hydrolysis rate coefficients and degradability fractions and maximum biomethane potential determined using

the linear and non-linear parameter estimation methods. In all the different cases, the biodegradability coefficients were estimated and provided insight on the characterization of the substrates. For instance, the degradability extent for fish waste silage was 84 %, while the degradabilities of cow manure, seed fish sludge and biosludge were 41 %, 64 % and 18 %, respectively. While the anaerobic digestion of fish waste silage is expected to result in a high biogas production, the results show slow degradation kinetics with a hydrolysis rate coefficient of 0.17 d^{-1}. Thus, it is important to mention that the hydrolysis rate coefficients k_{hyd} were very low as typical for BMP tests. By contrast, the degradation of substrates in full-scale systems estimated with gas flow as fitted data has been demonstrated to be much faster and showing higher degradability than the BMP tests (Batstone et al., 2009). To have the model reflect the reasonably fast dynamics of anaerobic digestion, a value of k_{hyd} of about 4 day^{-1} was used in the calibration of the digester process unit.

Table 6. Summary of the hydrolysis coefficients, degradability fractions and the maximum biomethane potential for fish waste silage, cow manure, seed fish sludge and biosludge.

Co-substrate	k_{hyd} (d^{-1})	f_d (%)	B_0(mL CH_4.gVS^{-1} day^{-1})
Fish waste silage	0.36±0.01	84±0.4	632±3.62
Cow manure	0.51±0.01	41±0.1	188±0.45
Seed fish sludge	0.78±0.01	64±0.1	471±0.66
Biosludge	0.17±0.01	18±0.2	91.4±1.6

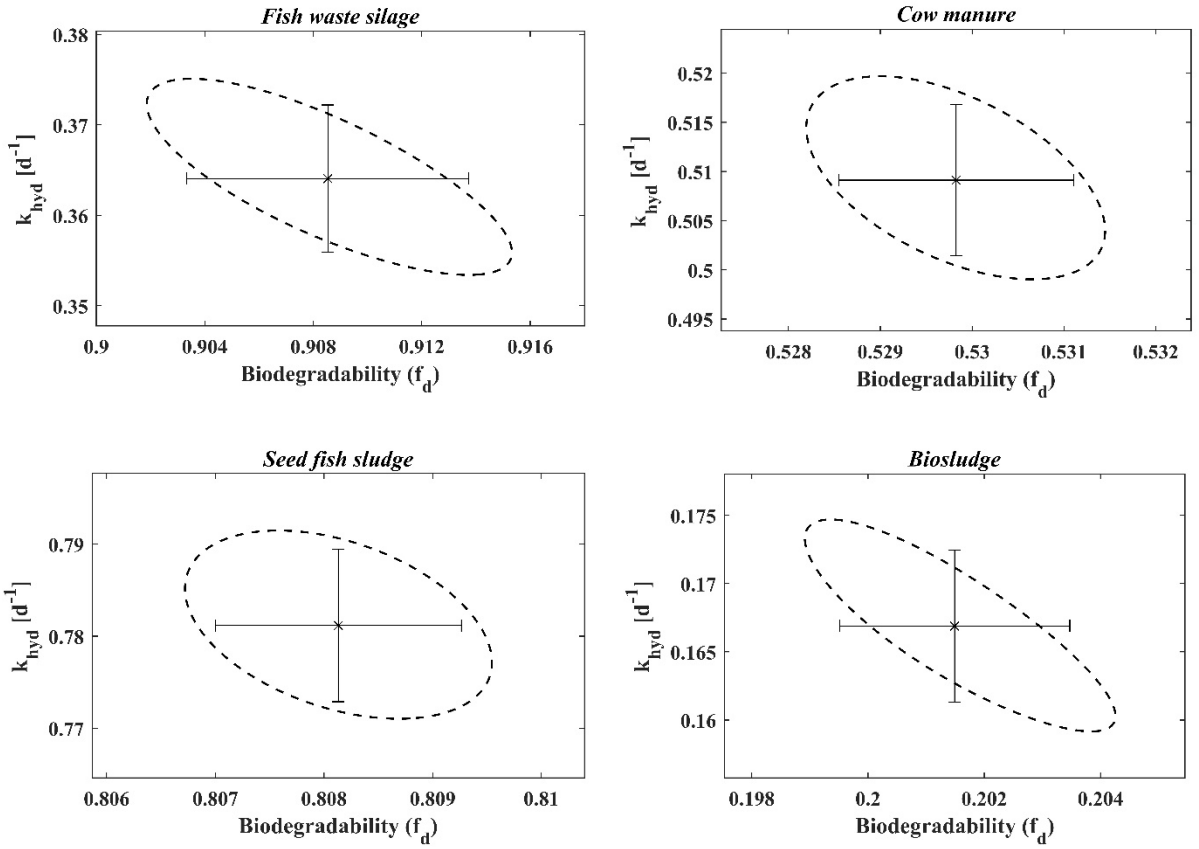

Figure 4. Confidence regions (95 % confidence limit) for the estimated degradability (f_d) and hydrolysis coefficient (k_{hyd}) for the biomethane potential test for the main co-substrates (fish waste silage, cow manure, seed fish sludge and biosludge).

Using the biodegradability (f_d) determined above and the compositional analysis of substrates, the COD, total nitrogen and total phosphorus were fractionated according to the methodology used for influent characterization. Table 7 shows the various COD, N and P fractions for the co-substrates. The estimated organic matter contents included a significant amount of readily biodegradable substrates, but the VFA levels were very low in comparison to the total COD. The co-substrates also contained high levels of the particulate unbiodegradable organic fractions, which were used as one of the calibration parameters for total suspended solids in the anaerobic digesters.

Table 7. Average steady-state co-substrate composition used for steady-state model calibration and validation.

Parameter	Fish silage	Cow manure	Seed fish sludge
VFA (g COD.m^{-3})	19.8	0	0
Readily biodegradable substrate (gCOD.m^{-3})	163 000	2 560	32 900
Colloidal biodegradable substrate (gCOD.m^{-3})	22 800	14 200	4 460
Slowly biodegradable substrate (gCOD.m^{-3})	281 000	39 600	50 700
Soluble unbiodegradable organics (gCOD.m^{-3})	29 000	17 800	4 220
Colloidal unbiodegradable organics (gCOD.m^{-3})	5 710	3 560	1 120
Particulate unbiodegradable organics (gCOD.m^{-3})	81 600	12 600	46 000
Total ammonia (NHx) (gN.m^{-3})	1 640	1 980	0
Soluble biodegradable organic N (gN.m^{-3})	6 500	102	1 310
Particulate biodegradable organic N (gN.m^{-3})	8 910	165	4 270
Particulate unbiodegradable organic N (gN.m^{-3})	816	126	459
Orthophosphate (PO_4) (gP.m^{-3})	2 590	254	966
Soluble biodegradable organic P (gP.m^{-3})	244	25.6	65.7
Particulate biodegradable organic P (gP.m^{-3})	502	237	24.7
Particulate unbiodegradable organic P (gP.m^{-3})	81.6	12.6	0

3.3 Dynamic plant influent

The purpose of fitting a simplified influent generator model to full-scale plant data was to provide a representative input for dynamic simulation assessments. Figure 5 displays representative full-scale data over 365 days (1 September 2018 to 31 August 2019), together with the influent model generation for flow rate and COD. The influent generator provided modelled data at 1 h intervals, whereas routine plant measurements were relatively sparse with sampling and analysis weekly or a few days a week. Simulation results of COD are mostly in good agreement with measured data, with a relative difference of 4.14 % between them. Larger short-term discrepancies can be seen (e.g. around day 205). These are related to larger production changes or service stops at the mill which are not included in the influent generation. For the purpose of dynamic simulations similar disturbances and other anomalies were not considered relevant to simulate considering the objective of the study. The high-frequency profiles of TKN, TP and TS were produced on the same basis as the COD, however the plant did not have long-term measured data for these components for validation. Therefore, the soluble organic components and nutrients were determined using the static influent characteristics, whereas the cation and anion concentrations were assumed to be constant. The dynamic influent data was used to investigate subsequent scenario analyses for the industrial symbiosis under study. Time-varying inputs of flow or concentrations were not available for the co-substrates, thus uniform compositions were used in the dynamic simulations.

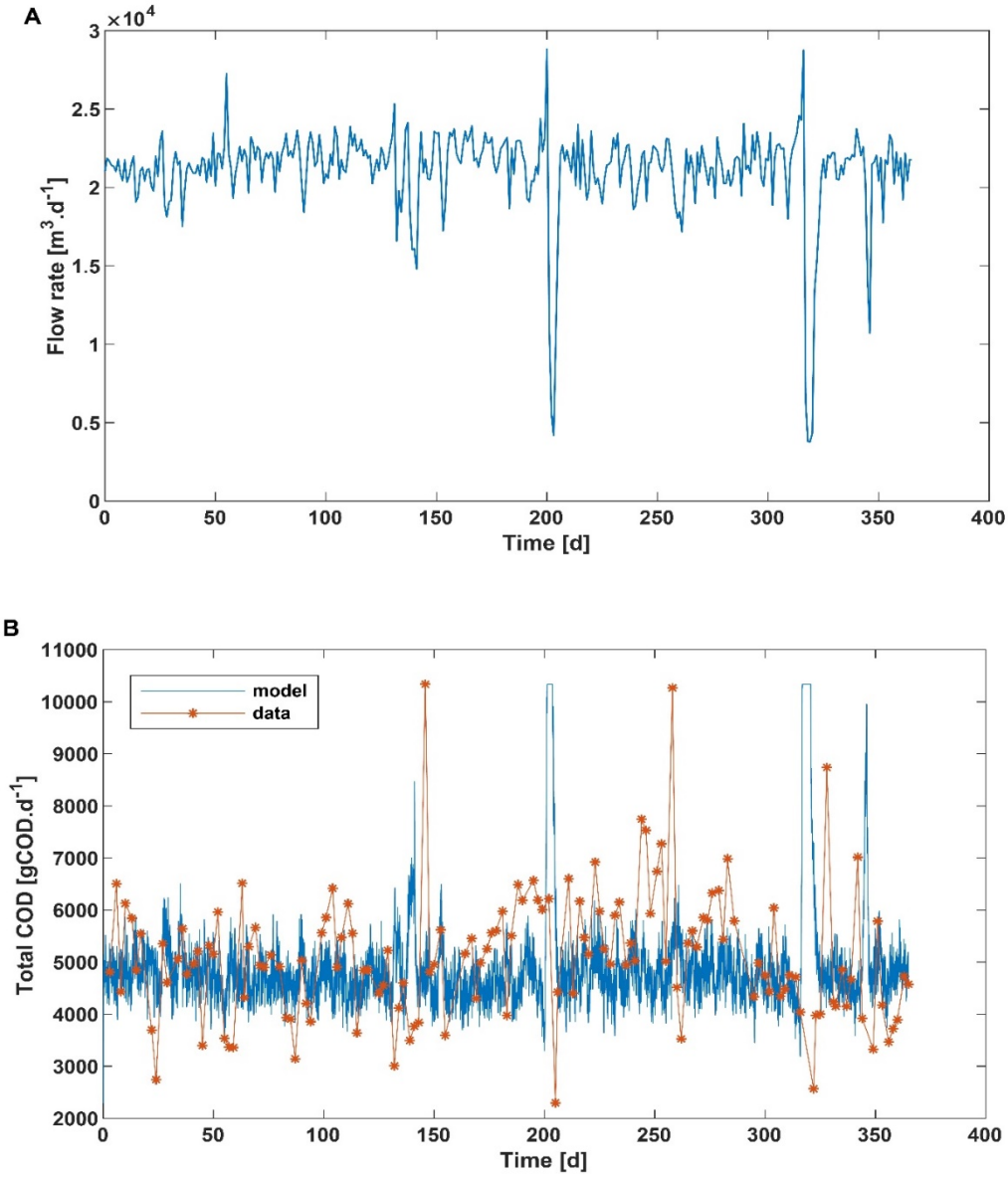

Figure 5. Dynamic plant influent for representative measured (A flow rate) and modelled and simulation data (B Total COD).

3.4 Plant steady-state analysis

3.4.1 Model calibration

The model evaluation encompassed a validation of its general capability to describe the wastewater, sludge and gas lines at different points along the interlinked treatment plants at steady state. For example, the calibration of ASS consisted of fitting all the effluent quality concentrations (N, P and COD), sludge production and oxygen demand to full-scale plant data by primarily adjusting the wastewater characteristics. The integrated model is complex and very parametrised, however, only a few kinetic and stoichiometric parameters had a significant impact on the calibration of the activated sludge and anaerobic sludge models as displayed in Table 8. Some of the most influential parameters included the ordinary heterotrophic organism growth rate (μ_{OHO}), the heterotrophic yield (Y_{OHO}) in the activated sludge system and the hydrolysis rate in the anaerobic digestion model. The values for decay rates and half

velocity coefficients for heterotrophs were within the limits reported in the literature (Barker and Dold, 1997; Henze, 2000). However, the maximum growth rate and growth yield values were lower than literature reported values. One reason for the difference might be that compositions of the mill wastewater is highly different from municipal wastewater (Brault et al., 2010; Lindblom et al., 2004). The rates of mineral precipitation were adjusted to calibrate key nutrients (P and N) in the reject water. These minerals included calcium carbonate, calcium phosphate and struvite. The level of sulphide in the anaerobic digesters was calibrated via the precipitation rate of iron sulphide (FeS).

Table 8. Process kinetics and stoichiometry of key parameters in the integrated model.

Name	Default	Value
Maximum specific growth rate of OHOs, μ_{OHO} (d^{-1})	4.0	4
COD of biodegradable substrate in volatile solids, $i_{CV,XB}$ ($gCOD.gVSS^{-1}$)	1.8	1.92
COD of biomass in volatile solids, $i_{CV,BIO}$ ($gCOD.gVSS^{-1}$)	1.42	1.42
Maximum specific growth rate of AOBs, μ_{AOB} (d^{-1})	0.85	0.25
Maximum specific growth rate of NOBs, μ_{NOB} (d^{-1})	0.65	0.15
Decay rate of AOBs, b_{AOB} (d^{-1})	0.17	0.17
Yield of OHOs on readily biodegradable substrate under aerobic conditions, $Y_{OHO,SB,ox}$ ($gCOD_{biomass}.gCOD_{substrate}^{-1}$)	0.67	0.5
Rate of struvite precipitation, k_{STR} ($g.m^{-3}.d^{-1}$)	10	0.035
Rate of ACP precipitation, k_{ACP} ($g.m^{-3}.d^{-1}$)	5	0.045
Rate of CaCO3 precipitation, k_{CaCO3} ($g.m^{-3}.d^{-1}$)	0.1	0.75

3.4.2 Steady-state model validation

A steady-state validation of the plant-wide model was carried out with the calibrated parameters using Dataset 2. Figure 6 presents steady-state experimental and simulated data for selected key variables and shows a good general agreement between the measurements and the model predictions. As expected, the model was able to predict the biogas production and concentrations of P, N, CH_4 and COD. For the steady-state scenario, differences between measured and modelled biogas flow of 2-3.2 % were observed for the ECSB and CSTR and the plant-wide prediction errors for NH_4-N and PO_4-P release were roughly 5.3 % and 7.4 %, respectively. The relative error for measured and predicted ammonia nitrogen, nitrate, phosphate and COD in the plant effluent were 1.3 %, 1.8 %, 0.9 % and 3.8 %, respectively.

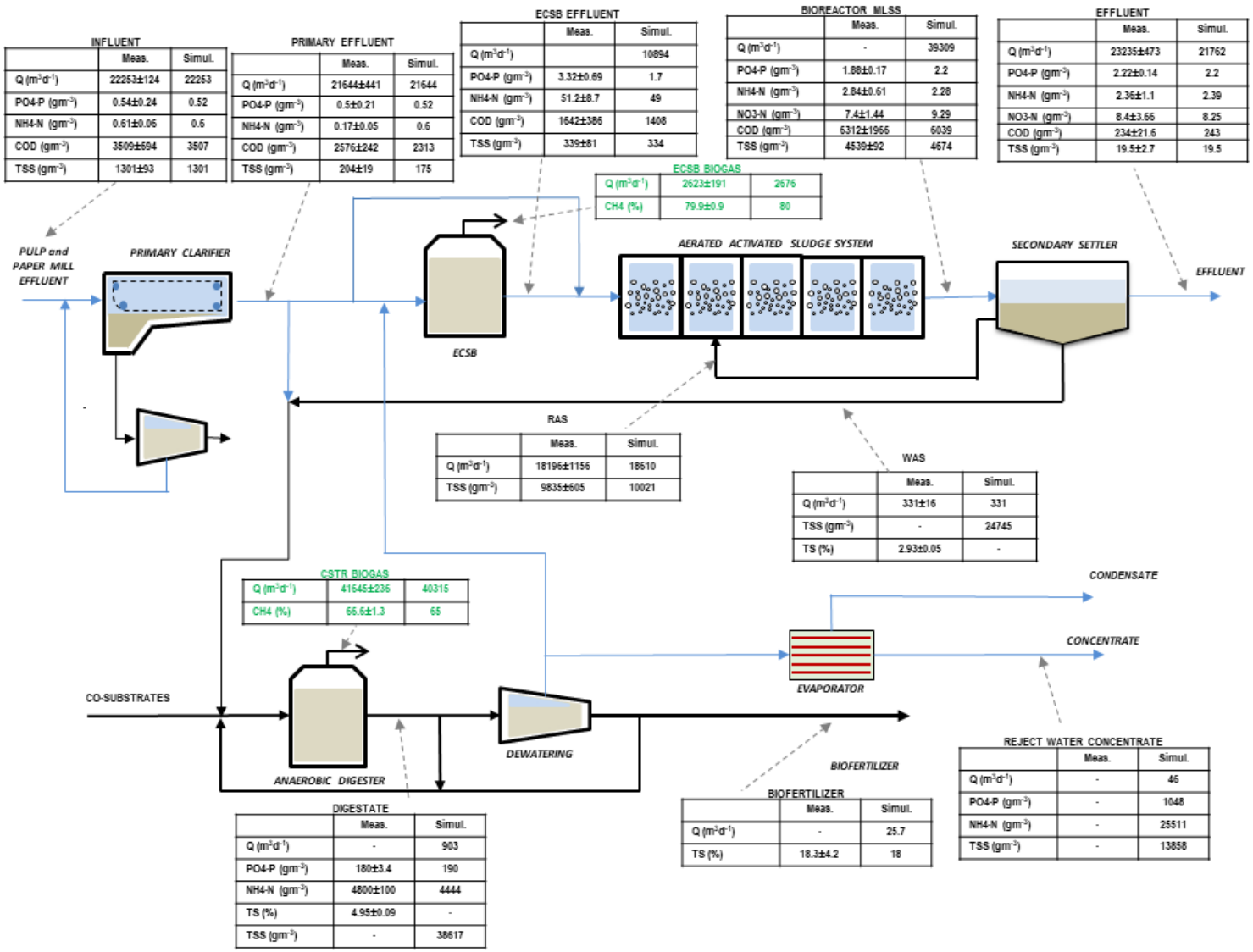

Figure 6. Steady-state comparison of the model predictions and measured data for representative streams and variables across the industrial symbiosis system.

Mineral precipitation played a key role in calibrating NH_4-N and PO_4-P in the reject water being recycled upstream the ECSB plant. Higher pH values and lower concentrations of divalent cations (Mg^{2+}, Ca^{2+}) indicate that $CaCO_3$, $Ca_3(PO_4)_2$ and $MgNH_4PO_4$ were the competing and dominant minerals in the digesters.

Steady-state results indicate that the dynamic process behaviour can be described accurately with a simplified ECSB, a standard activated sludge model and a simple (two-population model) anaerobic digestion models combined with a sophisticated pH and mineral precipitation model.

3.4.3 Model-based analysis of conversion of sulphur

Influent sulphur lies as sulphate (SO_4) about 100 $gS.m^{-3}$ + 15 $gS.m^{-3}$ other forms adding up to 115 $gS.m^{-3}$ or 2 577 $kgS.d^{-1}$. The co-substrates for the CSTR has a total sulphur (TS) concentration of 3 100 $gS.m^{-3}$ which adds another 470 $kgS.d^{-1}$. No other substantial additions of sulphur are made to the plant, e.g. from chemicals, etc. In total, the plant receives 3 050 $kgS.d^{-1}$. Influent and effluent mass flows of sulphur is presented in Table 9.

Table 9. Mass flows of sulphur compounds in the plant influent and effluents. TS denotes total sulphur.

	Influent WW	Influent co-substrates	ASS off-gas	Plant effluent	Bio-and primary sludge	CSTR sludge	Evaporator conc.	Evaporator effluent
TS ($kgS.d^{-1}$)	2 580	472	–	1 750	191	165	30	12
SO_4 ($kgS.d^{-1}$)	2 210	87	–	1 720	18	0.10	0.86	0.34
H_2S ($kgS.d^{-1}$)	1.6	0.15	363	0.0028	0.0063	0.29	2.4	0.95
FeS ($kg.d^{-1}$)	–	–	–	–	–	423	54	21

In the water train, the influent WW is firstly and mainly treated anaerobically in the ECSB. There, the sulphate is reduced to hydrogen sulfide (H_2S) (in equilibrium with bisulphide HS^-), Table 10. Some of this will be stripped with the biogas. The hydrogen sulfide concentration of the ECSB biogas is 1.7 % (v/v). The soluble hydrogen sulfide exiting the ECSB system will enter the aerated reactors in the ASS. First the free swimmer step in Selector 2 followed by Selector 1, partly 3, 4 and finally 5. From Selector 1 and downstream (i.e. facilitated by RAS) there are favorable conditions for sulfide oxidizing organisms (SOO) and oxidation back to sulfate is mediated (Table 10). However, in Selector 2 and partly also in Selector 1 the concentration of hydrogen sulfide is relatively high – 53 and 11 $gS.m^{-3}$ respectively – and some is stripped with the forced flow of air through the reactors. The model predicts 312 and 50 $kgS.d^{-1}$ being stripped in Selector 2 and 1, this corresponds to 15 % of the ASS influent TS (Table 9). The oxidation of H_2S to SO_4 by SOO is a two-step process via elemental sulphur, S^0. Elemental sulphur remains at elevated concentrations in Selector 2 and 1 but are negligible in the ASS effluent (Table 10) indicating that there is a high reaction rate in these first reactors and that the reactions cannot be complete. However, this S^0 is oxidized all the way to sulfate by the end of Selector 5. In Selector 5 all hydrogen sulfide is converted to sulfate apart from the fraction that is assimilated with the biomass.

In the sludge train the influent TS, mainly from co-substrates, also enters an anaerobic reducing environment in the CSTR digester. However, in the CSTR FeCl is dosed which largely

fix the sulphide as FeS (s). The H_2S content in the gas is low, 0.057 % (v/v), and also the soluble H_2S concentration in the reject water from the sludge dewatering is low, 9.2 $gS.m^{-3}$.

As presented in Table 9, at the plant effluent 1 750 $kgS.d^{-1}$ remains of the influent sulphur corresponding to 57 % of the total influent of TS (or 68 % of the WW influent). 1 300 $kgS.d^{-1}$ is removed over the plant. Out of the removed TS, 165 $kgS.d^{-1}$ lies in the CSTR sludge and 191 $kgS.d^{-1}$ in the thickened primary and WAS sludges. A smaller part exits the plant with the evaporator concentrate and permeate (about 40 $kgS.d^{-1}$). The rest is stripped, from the ASS (about 360 $kgS.d^{-1}$) and the biogas.

Table 10. Concentrations of sulphur compounds in selected parts of the water train. TS denotes total sulphur.

	Influent WW	ECSB effluent	Selector 2	Selector 1	Selector 5	Plant effluent
TS ($gS.m^{-3}$)	116	102	85	99	99	80
SO_4 ($gS.m^{-3}$)	99	3.8	20	51	79	79
H_2S ($gS.m^{-3}$)	0.07	92	53	11	0.0001	0.0001
S^0 ($gS.m^{-3}$)	–	0.0031	4.8	15	0.0027	–

3.5 Analysis of model scenarios

3.5.1 Impact of sludge age – Scenario 1 and 2

The treatment of pulp and paper mill effluents by the activated sludge process is cost- and energy intensive due to the need of oxidising a large fraction of organic matter to CO_2 and subsequent management of sludge. Short sludge age has been proposed as an efficient way of reducing the cost associated with aeration (Jimenez et al., 2015). In this regard, simulations were carried out with the calibrated model to study the impact of reducing the sludge age from 17 days to 8 days. Table 11 shows the mass flows of some variables in the waste activated sludge for scenario 1 and scenario 2. In general, the mass flow of organic components in the WAS increased when the sludge age decreased from 17 days to 8 days. For example, the total COD mass flow increased by 16 % and the VSS mass flow increased by 13 %. The mass flow for slowly biodegradable organics also increased by 84 % when the SRT was decreased from 17 days to 8 days. The degradation of these slowly biodegradable organics by the OHOs is therefore related to the sludge age of the system with longer SRTs leading to complete mineralization of the biodegradable organics (only unbiodegradable soluble COD remains in the effluent). The activated sludge system operating at 17 days sludge age allowed the endogenous process to approach completion thereby achieving a low active fraction with limited anaerobic degradability.

The slowly biodegradable particulate organics at very short sludge age are not completely biodegraded but become enmeshed within the activated sludge flocs and become part of the suspended VSS sludge mass in the reactor. Hence treatment of wastewater at short sludge age minimizes biological oxidation instead capturing organic carbon in the sludge by adsorption, particulate enmeshment, bio-flocculation, accumulation and assimilation (Jimenez et al., 2005).

Table 11. Mass flows of some variables in the waste activated sludge for scenario 1 and scenario 2.

Variable mass flow in WAS	Scen1 - SRT 17 days	Scen2 - SRT 8 days
COD ($kg.d^{-1}$)	8 790	10 200
TSS ($kg.d^{-1}$)	7 000	8 000
VSS ($kg.d^{-1}$)	6 600	7 470
BOD_5 ($kg\ O_2.d^{-1}$)	401	749
Slowly biodegradable substrate ($kgCOD.d^{-1}$)	22.8	42.0
Soluble unbiodegradable organics ($kgCOD.d^{-1}$)	68.3	244
Particulate unbiodegradable organics ($kgCOD.d^{-1}$)	7 140	7 210
Total nitrogen ($kgN.d^{-1}$)	148	233
Total phosphorus ($kgP.d^{-1}$)	48.3	73.1
Total sulphur ($kgS.d^{-1}$)	76.5	152
OHO ($kgCOD.d^{-1}$)	1 000	1 880
Endogenous decay products ($kgCOD.d^{-1}$)	436	605

3.5.2 Nutrients dosage optimization – Scenario 3

The impact of implementing a basic control and operational strategy for dosing ammonia nitrogen and phosphate, required for microbial activity while maintaining the concentrations of these dissolved macro-nutrients below the required levels in the effluents, was investigated (Scenario 3a (17 days SRT) and 3b (8 days SRT)). It is known that insufficient nutrient levels are detrimental to microbial growth. On the other hand, overdosing is undesirable because it may violate the discharge limits and increase the operational costs and carbon footprint of the WWT. Table 12 displays the results of the optimization of nutrients dosage. The results show that the amount of chemicals (in this case only H_3PO_4) dosed can be completely removed at a sludge age of 17 days (scenario 3a) while in the scenario 3b a small addition of phosphoric acid is still needed while keeping a sufficient nutrient level in the activated sludge treatment and a desired effluent quality. Also, the amount of nitrogen, supplied only by the reject water, could be reduced. For example, 639 kg N from the reject water was dosed in Scenario 1, but only 531 kg N was needed during optimization in scenario 3a (SRT: 17 days), indicating a reduction of about 18 % of N (Table 12). Regarding phosphorus addition, a dosage reduction of 66 % was observed when addition was optimized. This meant that no H_3PO_4 had to be added and that all the P could be gained from the reject water at 17 days sludge age (Table 12). The trend was similar for scenarios 2 and 3b (with sludge age of 8 days). In this case, the reduction of the amounts of N and P needed in the process and supplied via reject water and H_3PO_4 were 7 % and 41 % for Scenario 3b compared to Scenario 2. These results show that the extent of nutrient dosing could be related to the SRT of the activated sludge system. For instance, an activated sludge treatment plant with a longer SRT (Scenarios 1 and 3a) is associated with higher concentrations of microorganism in the biomass which in turn may release nutrients due to extended mineralization. In contrast biomass decay and nutrients release are limited at lower sludge ages as also indicated in Section 3.5.1.

Table 12. Steady state optimization of chemicals dosing to the ECSB and activated sludge systems (urea was not added). The H_3PO_4-A refers to the dosing point prior the ESCB and H_3PO_4-B to the dosing point between the ECSB and ASS.

Scenario	Nutrient dosing				Effluent quality		
	N reject water ($kgN.d^{-1}$)	P reject water ($kgP.d^{-1}$)	H_3PO_4-A ($kgP.d^{-1}$)	H_3PO_4-B ($kgP.d^{-1}$)	N ($kgN.d^{-1}$)	P ($kgP.d^{-1}$)	COD ($kgCOD.d^{-1}$)
Scen. 1	639	44	9.1	52	126	73	5 334
Scen. 2	635	47	9.1	52	125	52	5 322
Scen. 3a	531	36	0	0	110	12	5 282
Scen. 3b	588	43	0	20	122	12	5 304

The results indicate that optimizing N and P loading at the ECSB or ASS is essential for growth of microorganisms and can, in this case, to a large extent be achieved with recirculated reject water. However, it is worthwhile mentioning that digester supernatant or reject water may be a major internal load as far as nutrients recycling within the industrial symbiosis is concerned, especially concerning ammonia nitrogen, particularly when proper optimization is not carried out. This can lead to increased nutrient concentrations in the effluent, well above the limits. While the recirculation of the reject water to the head of the ECSB and activated sludge system plays a significant role in supplying key nutrients, care should be taken to ensure the effluent quality limits are met.

3.5.3 Plant-wide dynamic response – Scenario 4

In order to demonstrate the usefulness and application of the plant-wide model of this industrial symbiosis concept, several dynamic scenarios were set up in which transient behaviours of the system were considered as a result of step changes or bypass of influent over the ESCB to simulate disturbances that may result for instance from high TSS concentrations in the primary settler over-flow. The effects of bypassing the ECSB were investigated as part of Scenario 4. Here 100 % of the flow was bypassed at day 5, day 22.5, day 49, day 86 and day 142 from simulation start and for a duration of 0.5, 1, 3, 5 and 7 days, respectively.

Figure 7a shows the primary effluent and the flow to the ECSB, together with the comparison of the impact of bypass on MLSS in the activated sludge system (Figure 7b and Figure 7c). As expected, bypassing the flow to the ECSB increased the concentration of suspended solids in the activated sludge system and decreased it again once 90 % of the primary effluent flow was fed again to the ECSB (sludge wastage rate from the ASS was kept constant). The time response depended on the duration of the bypass with a short bypass resulting in rapid recovery while longer response times were seen for prolonged flow bypasses. The flow bypass caused a step change in COD concentrations, which in turn increased the food supply (readily biodegradable COD) causing an increase in the heterotrophic biomass population (up to about 30 % for the bypass scenarios simulated). The additional volumetric loading also caused the inert particulate COD (and consequently the MLSS) to increase in the activated sludge system.

Figure 8a shows the impact of biogas production in the ECSB as a result of influent bypass, where the withdrawal of the relatively COD-rich water from the ECSB gives a clear negative effect on the biogas production. As a result of the bypass of the ECSB reactor, the untreated wastewater is instead fed directly into the ASS causing an increase in the load of total COD as can be seen in Figure 8b The increased load will mean an increased number of heterotrophs which in turn mean more decayed heterotrophic biomass that, in turn, resulted in higher

organic nitrogen released to the system. The increased influent rate during by-pass resulted in an increase in the mass of ammonia introduced to the aeration basin (ammonia influent concentration was the same but since the flow was higher, the mass-flow of ammonia was higher too), that in turn increased the ammonia concentration in the ASS. More ammonia could mean more food for the autotrophic population, i.e. increase in the biomass growth. However, the effluent phosphorus concentration was significantly reduced after an initial spike in phosphate resulting in increased values the day when the by-pass was initiated in each case. The simulations with intervals of bypassing showed, for 17 days sludge age, that by-pass times of 0.5 to 1 day did not give COD or NH_4-N releases above 13 700 and 400 kg per day respectively (discharge limits) while 3, 5 and 7 days by-passes resulted in higher daily releases (Figure 9d and 9e). There was however a delay in the release in NH_4-N compared to when each by-pass was started (Figure 10), so when the by-pass was initiated day 49 (3 days by-pass) the increase in levels of NH_4-N above 400 occurred days 52 to 54, while when the 5 days by-pass was started at day 86, NH_4-N above 400 was predicted for days 91 to 95 and for the final by-pass (7 days from 142) NH_4-N-values above 400 was registered for days 149-155. The by-pass time was also shown to influence the duration of the disturbance with 3 days bypass resulting in daily discharge levels above 400 for three days while 5 days by-pass gave five days with levels above 400 and 7 days by-pass gave seven. The same pattern could be observed for the COD releases, thus giving levels above 13 700 for 3, 5 and 7 days respectively but here the increase in COD came quicker with, reaching levels above the discharge limits only one day after the start of the by-pass respectively.

Figure 9 shows the results for the step change dynamic simulations for scenarios 2 and 4b at 8 days of sludge age. The model responses are the same as to those in Scenarios 1 and 4a (17 days of sludge age) and demonstrated again that the time constants for the dynamic model responses depended on the nature of the imposed step change. In general, the response of a step change in the influent flow to the ASS was very quick for a short bypass, while that caused by a long step change was significantly longer than one day for all the variables. As previously, some model variables initially reacted quickly but required a long time to reach a steady state (COD, ammonia nitrogen), while some reacted quickly only to specific changes (e.g. P and pH).

Overall, subsequent recovery was obtained only when the COD loading was markedly reduced or when the system would reach a new semi-stable operating condition (not simulated).

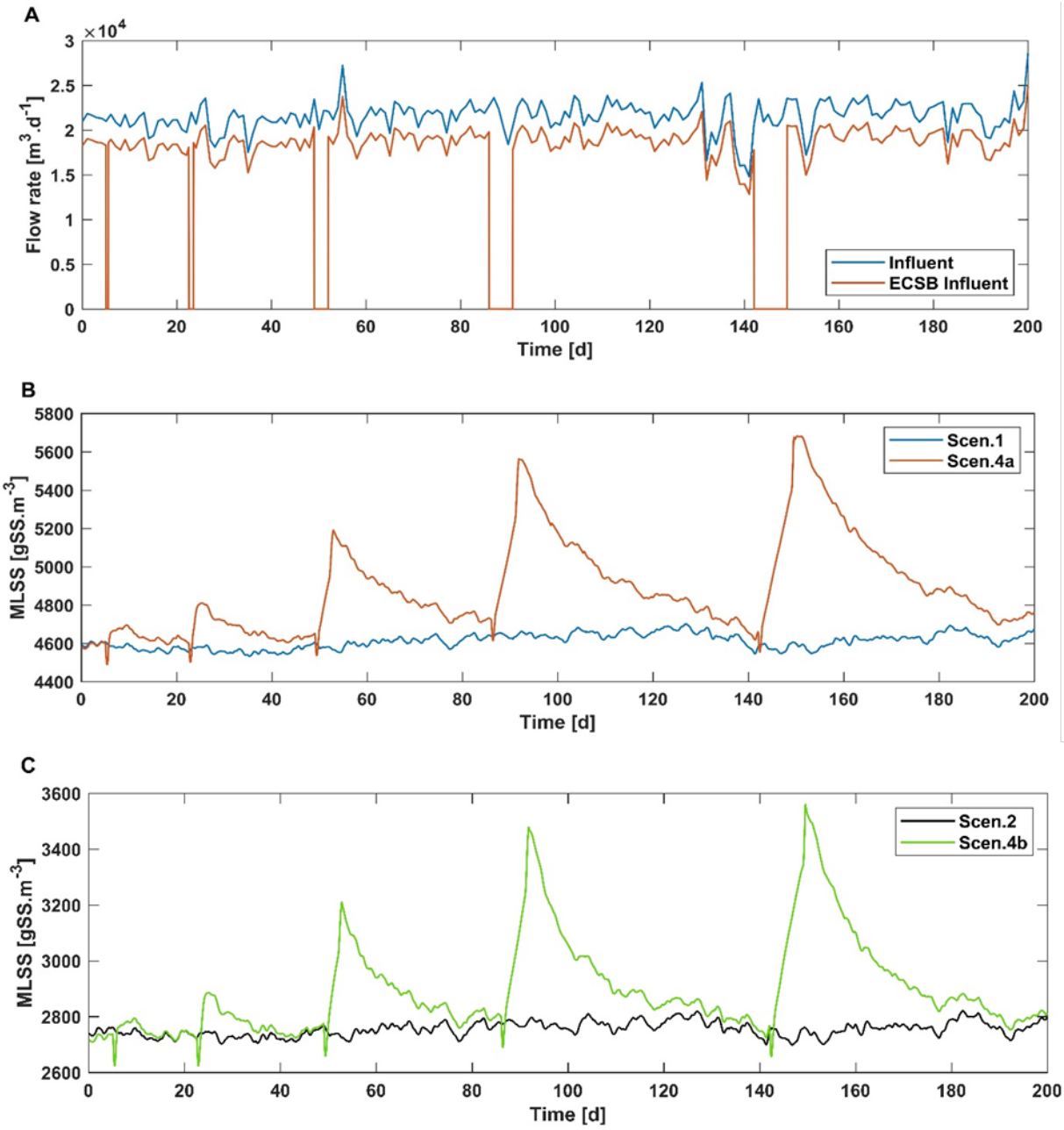

Figure 7. Primary influent and effluent flows to ECSB with the step changes or bypass (a), suspended solids in the mixed sludge for scenario 1 (17 days of sludge age) and scenario 4a (17 days of sludge age) with step changes (b), suspended solids in the mixed sludge for scenario 2 (8 days of sludge age) and scenario 4b (8 days of sludge age) with step changes (c). The effects of bypassing the ECSB were investigated as part of Scenario 4. Here 100 % of the flow was bypassed at days 5, 22.5, 49, 86 and 142 for a duration of 0.5, 1, 3, 5 and 7 days, respectively.

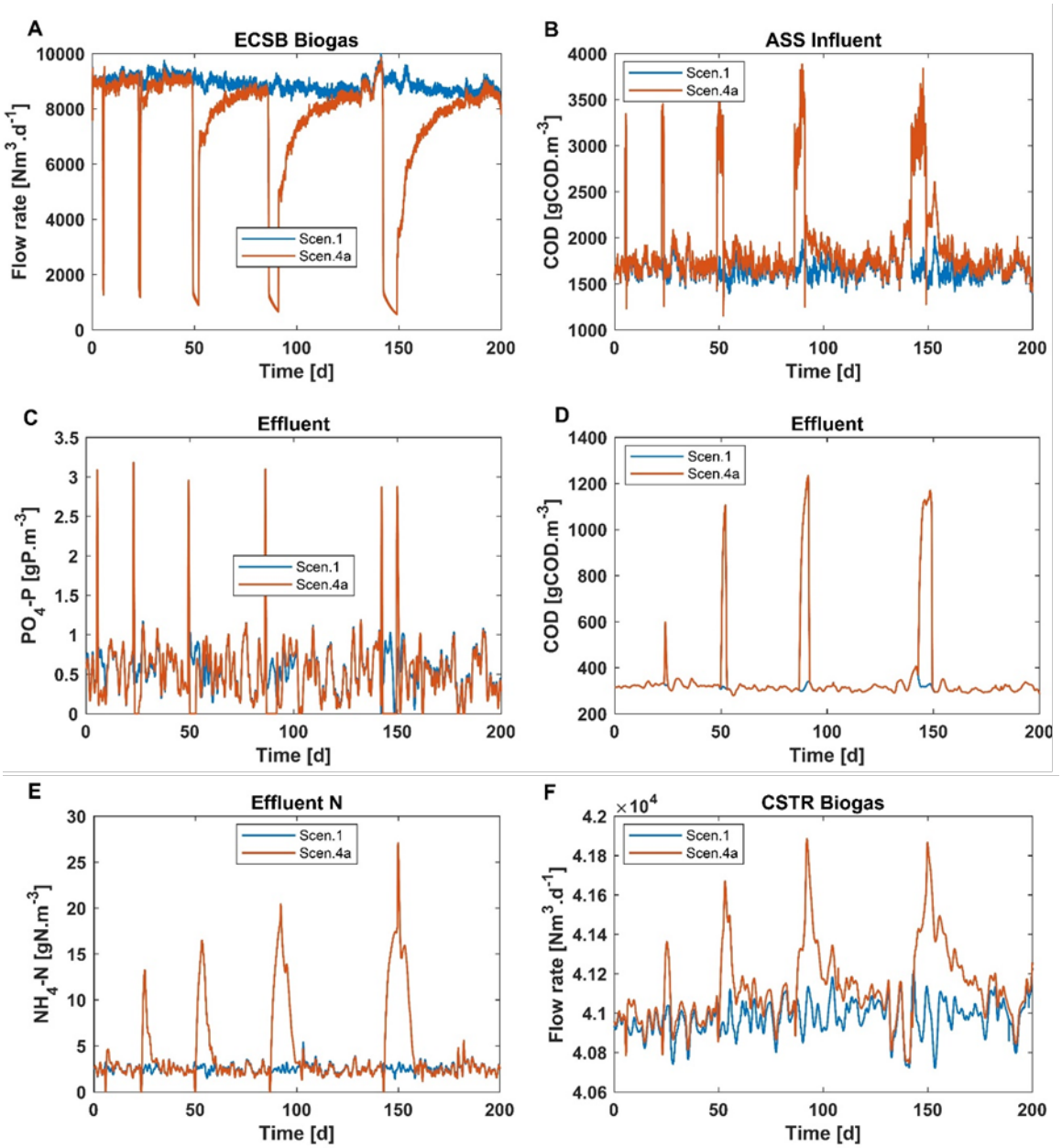

Figure 8. Step change dynamic simulations of selected parameters: ECSB biogas flow (A), COD concentration in the ASS influent (B), effluent soluble phosphate (C), effluent COD (D), effluent ammonia nitrogen (E) and CSTR biogas (F) for Scenarios 1 and 4a (17 days of sludge age). The effects of bypassing the ECSB were investigated as part of Scenario 4. Here 100 % of the flow was bypassed at days 5, 22.5, 49, 86 and 142 for a duration of 0.5, 1, 3, 5 and 7 days, respectively.

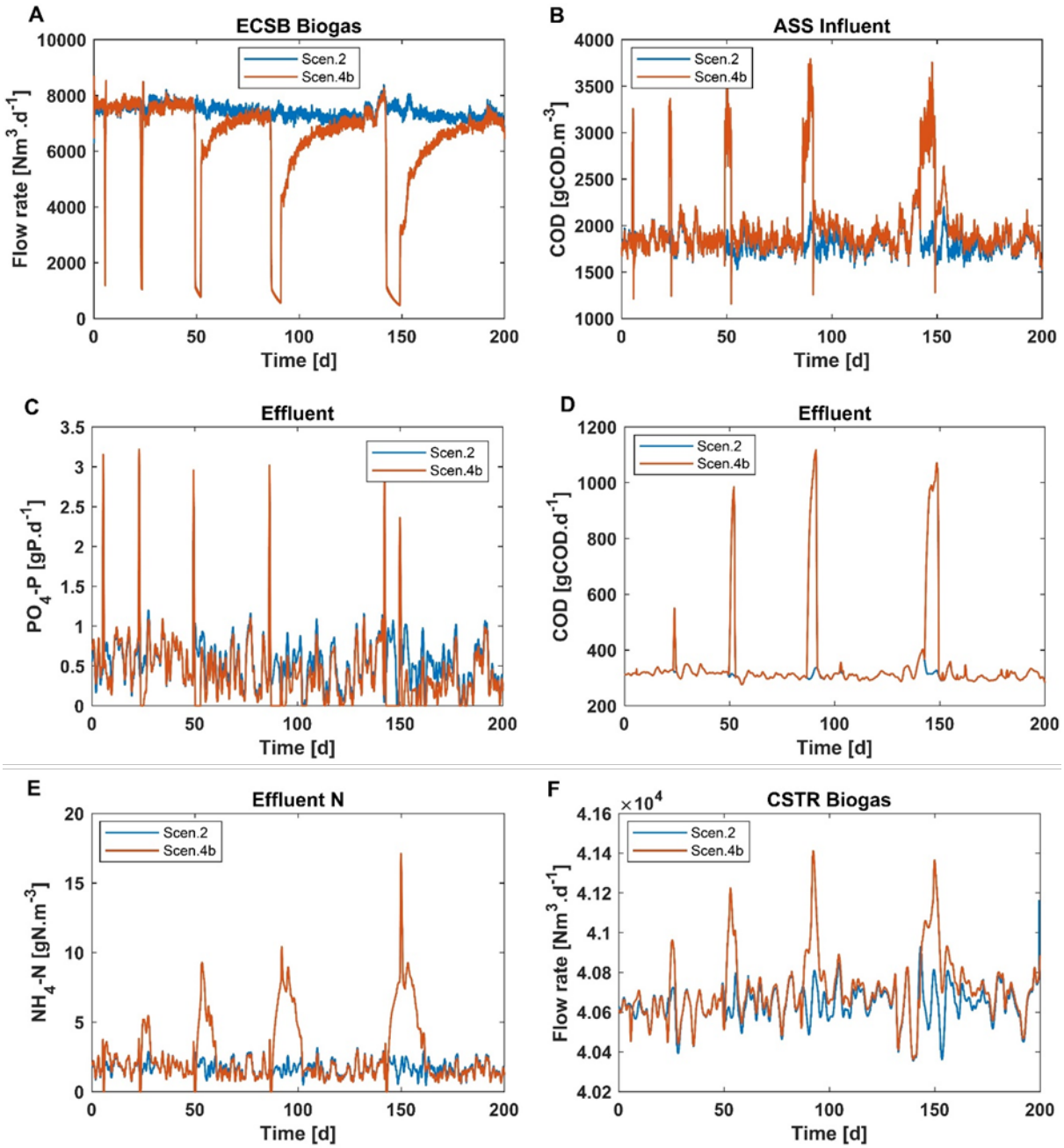

Figure 9. Step dynamic simulations of selected parameters: ECSB biogas flow (A), COD concentration in the ASS influent (B), effluent soluble phosphate (C), effluent COD (D), effluent ammonia nitrogen (E) and CSTR biogas (F) for Scenarios 2 and 4b (8 days of sludge age). The effects of bypassing the ECSB were investigated as part of Scenario 4. Here 100 % of the flow was bypassed at days 5, 22.5, 49, 86 and 142 for a duration of 0.5, 1, 3, 5 and 7 days, respectively.

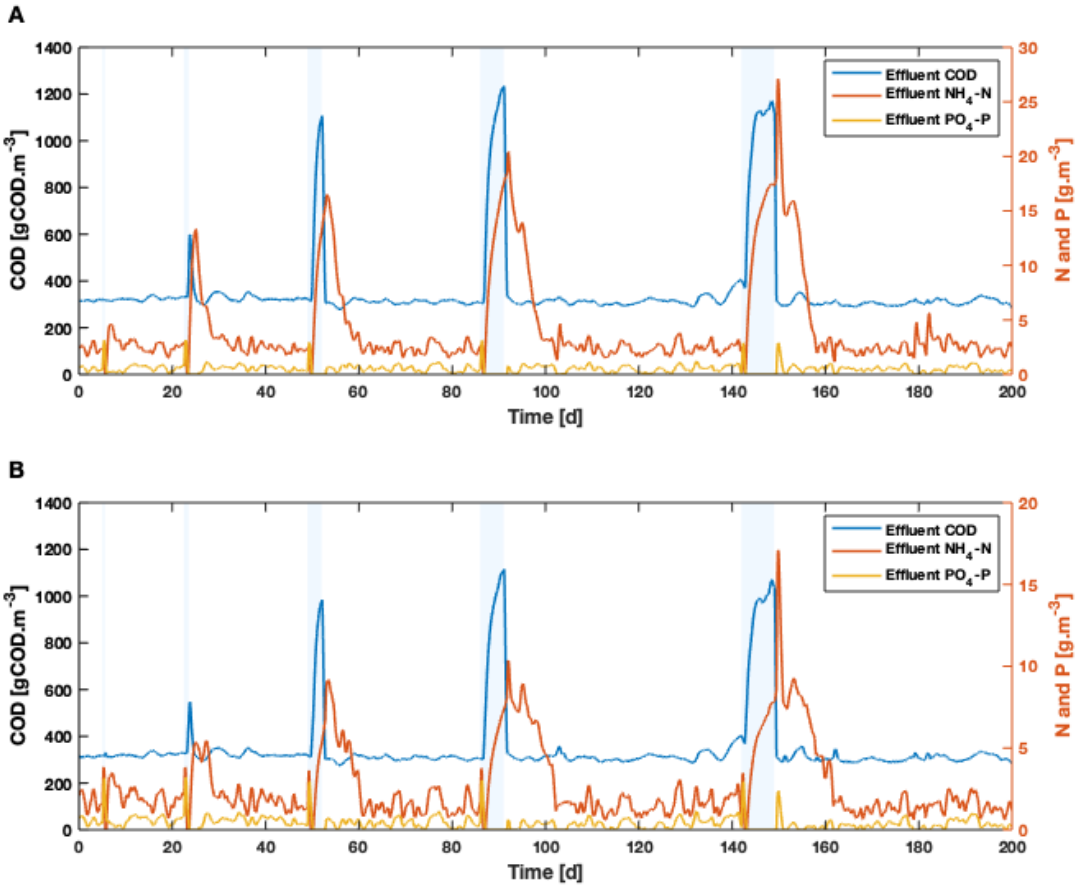

Figure 10. Effluent concentrations of COD (blue), NH_4-N (red) and PO_4-P (yellow) for scenario 4 with (A) 17 days of sludge age; (B) 8 days of sludge age. Shaded areas mark time and duration for the 5 bypass events.

4 Discussion

4.1 Model performance and use

This work has developed and integrated a modelling tool, capable of assessing the dynamics and interactions within an industrial symbiosis connecting an anaerobic high-rate system for pulp and paper mill effluent treatment, an ASS and CSTRs for anaerobic co-digestion whereby rejected water from final dewatering at the CSTRs serves as nutrient supply upstream. The model includes sub-models for all relevant processes so that the mass balance and dynamics of organic material and nutrients between the systems can be simulated. For the system analysis, the model allows for multi-objective analysis: e.g. ASS and AD performance, effluent water quality, biogas production, resource recovery and resource use.

The model is able to:

- Predict the characteristics of the COD going into the ASS as a result of changes caused by the inclusion of a high-rate anaerobic step before the ASS. The VFA and readily biodegradable organics are mostly removed in the ECSB, while the slowly biodegradable organics undergo degradation and mineralisation by the heterotrophs in the activated sludge system. This means that the load on ASS is reduced substantially and that a by-pass of selector 3 can be performed without risks in overloading the ASS. The lower load also means a reduced need of aeration over the ASS.
- Predict how the sludge age in the ASS will affect the mass flow of biodegradable organics in the WAS stream, with a lower sludge age giving a higher mass flow and thereby potentially a higher biomethane potential of the WAS. As shown in Table 11 the BOD will almost double (from 400 to 750 kg O_2.d^{-1}) and it increases also in relation to VSS (from 6 to 10 %) showing that the increase is "real" and not only an effect of an increased mass flow. Also, the slowly biodegradable COD is roughly doubled. These increases indicate an improved biomethane potential of the WAS and that so should be the case is also supported by previous experimental studies, which have indicated that larger amounts of activated sludge with increased biodegradability are produced in high rate activated sludge reactors (Ge et al., 2013; Ge et al., 2017).
- Optimize the additions of N and P to the ECSB and ASS at normal operation to obtain stable, well-functioning treatment processes while at the same time minimising the COD, N and P levels in the final effluent. This will in full scale mean large savings in reduced nutrient additions. Compared to a case without a biogas plant (scenario 0, data not shown) generating reject water such as the one described here the nutrient dosing from commercial chemicals is low already for case 1 and 2 as given in Table 12. Case 0 would mean a need to supply both urea and H_3PO_4 to the ASS in amounts of about 4000 kg of urea (40 %; corresponding to about 800 kg N) and 300 kg of H_3PO_4 (75 %; corresponding to about 80 kg of P) per day while already case 1 and 2 show no need of urea addition and a reduction in the need of H_3PO_4 addition with about 40 % (Table 12). The optimisation of the nutrient dosing shows a further decrease in the need of H_3PO_4 additions to, in case 3a 0 kgP.d^{-1} and in case 3b 20 kgP.d^{-1}, which means a reduction with 75 % compared to case 0. These reductions mean both economic savings and reductions in the environmental footprints of the wastewater treatment

plant by means of reducing the use of commercially produced nutrients. From these results it can also be concluded that N-concentration in the reject water is the factor deciding how much reject that can be added without risking an N-overload. This means that there can be a need to top up the nutrients supplied with the reject water with extra P for example when an increased build-up of biomass is acquired in the ESCB or in the ASS (for the latter for example during by-pass of the ECSB).

- Predict the effect of ECSB-bypass on the ASS at different time length. Simulations of cases 4a and 4b showed up to one day's by-pass would give short peaks in phosphate (only one day duration) while not affecting the NH_4-N and COD concentrations much. 3, 5 and 7 days by-pass on the other hand gave levels of NH_4-N and COD above the discharge limits for a number of days. The pattern of the release was however different with a quicker COD peak and a more delayed NH_4-N release, see Figure 10. This phenomenon was due to the varying origin or processes causing the elevated concentrations. The COD peak resulted from influent overload of the ASS and was only delayed by hydraulics. The quick P-peaks that occur in the beginning to each by-pass is likely explained by a wash-out of decaying biomass from the semi-bypassed selector 3 of the ASS (in both scenario 1 and 2, 10 % of the flow through the ASS is led through selector 3 while the rest is bypassed from selector 1 to selector 4). The P-profile during bypass indicates that nutrient limitations occurred leading to biomass decay and thus limited the biomass capacity to handle spikes originating from bypasses in the present set-up. It should be noted that in Scenario 4, the nutrient dosing was at the optimized level (Scenarion 2). The P-release observed in the simulation indicates that the intentions of this by-pass i.e. to keep a "biomass buffer" ready to step in in case of increased loads to the ASS will not work as planned, at least not for preventing a release of P from the system. Furthermore, in the model decaying biomass in the ECSB during bypass events (primarily longer than one day) give rise to a similar wash-out of N and P to the ASS when the flow goes back to normal operation. Due to lack of data from similar events, it has not been confirmed in the project that this decay rate is coherent with a real situation. Considering that the ECSB has been modelled with a simplified apparent kinetics model approach rather than a proper granule sludge biofilm model, the real system could behave differently. The results show that the by-passes of the ECSB should be kept as short as possible but also that further tests are needed to try to revile and overcome the problems at longer by-passes.
- Predict the concentrations of sulphur compounds throughout the plant. The analysis of the sulphur conversions shows that most of the influent sulphur remains in the effluent WW. Some is removed with the withdrawn sludges and yet some is stripped with biogas and the airflow through the first two reactors of the ASS. The stripping in the ASS indicates that the concentration of HS^- fed to the ASS is too high, or the oxidation rate is too low, for all to be oxidized. Instead some is stripped. This result indicate that bad odours might arise at the plant. Regarding the H_2S in the biogas, the concentration is relatively high in the ECSB raw gas but in the CSTR most of the sulphur is fixed as FeS due to the dosage of FeCl.

4.2 Model Simplifications and Assumptions

The possibility to reduce energy input and enhance biogas production from pulp and paper mill wastewater COD is driving much interest in modelling high-rate anaerobic reactors, such as ECSB. The major difference between the ECSB model of those of other studies resides in the complexity of the hydrodynamics and the anaerobic digestion. While the ECSB model was able to predict the effluent COD, however, it fails to predict the granular mechanisms involving the three phases: (1) the solid phase consisting of bioparticles (granules) composed by active and non-active biomass, (2) the liquid phase containing the chemical species in aqueous solution (substrates, products, enzymes, ions and water) and (active and non-active) single suspended cells, which are assumed to behave as solutes and (3) the gas phase that contains the gaseous products from the anaerobic degradation. Depending on the objective of a study, modelling high-rate granular anaerobic processes may require a detailed description of the dynamics of these three phases (gas–solid–liquid) present in the reactor, biochemical, physico-chemical (i.e. mass transfers between the different compartments and phases) and hydrodynamic processes (Bolle et al., 1986; Costello et al., 1991; Fuentes et al., 2011).

Simulation results with step change scenario analysis show that the plant-wide model of an industrial symbiosis is a useful tool for predicting effluents and providing insight in the event of failures. One of the major limitations of an ECSB or any other high-rate granular sludge bed process is related to wastewaters having high suspended solids content, which hampers the development of a dense granular sludge. High concentrations of TSS in the influent can cause solids accumulation in the sludge bed, and consequently deterioration of sludge settleability and biomass washout (Richardson et al., 1991). Although the model does not consider complexity in terms of the nature of granular sludge in the ECSB, it was capable of adequately predicting the biogas flow in the system and downstream dynamics of COD and nutrients in the effluent in the presence of temporary disturbances. The accuracy of these predictions in terms of ECSB effluent concentration during and after a disturbance remains to be confirmed with measurements.

The secondary settlers are very simplified and does not capture the settling properties of the activated sludge. Further model refinements are therefore needed in order to improve the model prediction especially for special operational modes, such as high-rate systems (active sludge systems with one to three days sludge age).

A process of interest not included in the model is formation and consumption of methane in the ASS. In the investigated process configuration with anaerobic processes (ECSB in water train and CSTR in sludge train) upstream the ASS, dissolved residual methane will enter ASS. This is especially true for the ECSB as the flows are high. The fate of methane entering an ASS has been investigated (Daelman et al. 2012). It has been shown that both stripping but also biological degradation might take place simultaneously. These processes are not included or active in the ASS model. Neither is it known to which extent biological degradation of methane is taking place in the ASS under study. In a case where a significant amount of methane is biologically degraded, this impacts the microbial community, sludge production and oxygen consumption of the ASS.

4.3 Assessing Industrial Symbiosis and Model-Based Optimization

The overall results demonstrate that an integrated model is a suitable model for assessing industrial symbiosis for optimum production of biogas as well as nutrient concentrations in the system. Similar to what has previously been shown for municipal WWTPs (Arnell et al. 2016), the model allows for the prediction of nutrients release in anaerobic digestion and subsequent consumption upstream of the high-rate anaerobic system or activated sludge system and can therefore be used to develop, implement and assess realistic operational and control strategies. This study has demonstrated the necessity of imposing a basic control and operational strategy for efficient reject water recirculation to maintain optimum concentrations of N and P in the activated sludge system while also achieving nutrients level meeting the effluent permits.

Besides nutrients optimization, the model has the potential to assess other process optimization options, such as adding a new substrate to the ECSB or to the CSTR or evaluating the effects of gradually varying the load of one or more co-substrates of the CSTR on methane production. For example, the model can be useful in studying the effects of increasing the load of nitrogen-rich organic material on co-digestion and methane production, while predicting potential process disturbances due to transient overloading and accumulation of ammonia and volatile fatty acids.

5 Conclusions

A plant-wide model for an industrial symbiosis for biogas and pulp and paper mill effluent treatment plants was able to effectively predict as well as assess trends in a wide range of output variables including effluent quality (COD, ammonia nitrogen and phosphate), biogas flow and gas concentrations, nutrient release from the anaerobic digesters and their recirculation in the reject water to the ECSB and activated sludge systems. Discrepancies between the measurements and simulations were within the expected range of accuracy for complex integrated models.

To further validate the performance of the industrial symbiosis model, dynamic analyses were also performed. These indicated that the model can reliably describe the release and fate of nitrogen and phosphorus from the different sub-processes, such as CSTR, ECSB and activated sludge selectors during alternative operational modes. The effects described included their feedback effects on upstream plant performance via recycle streams and reject water recycling. The later impacted on the ability to provide not only enough nutrients for microorganisms, but also to achieve acceptable discharge nutrients limits. The results of dynamic response simulations indicated that the integrated model allows for analysis of total multiple criteria performance over time.

The model is general and extendable and can therefore be used for design and simulation of similar industrial symbiosis systems in different geographical locations, considering requirements for re-characterization of influents and re-calibration of model parameters. Plant operators can also use it to optimize and identify constrains in the treatment plant under various conditions, to allow them to evaluate, through simulation, the impact of different control and operational strategies and provide a tool for diagnosing operational upsets.

In more detail we, when applying the model on a number of scenarios linked to the case study, were able to show:

- A reduced need of nutrient dosing. The nitrogen additions could be reduced by 16 % comparing scenario 1 with scenario 3 and it was also shown that all nitrogen could be obtained from reject water, no urea additions was thus necessary. The phosphorous additions could be reduced with 66 %, also in this case could all or most of the P needed be obtained from the reject water depending on the SRT in the ASS. Thus, the amount of reject water supplied to the wastewater treatment will be limited by its N-content thus meaning that extra (commercial) P will have to be added especially when a build-up of biomass is needed in the ECSB and/or ASS. It should also be noted that compared to an ASS without the possibility to use AD-reject water the savings in dosing of commercial N and P are substantial.
- Impact of sulphur processes on AD and ASS. The high flows of sulphate in the plant influent WW largely remains in the plant effluent. Some of the total sulphur is fixed in the sludges and some is contained in the ECSB raw gas. However, a non-negligible amount is also stripped as hydrogen sulphide gas in the first two selectors of the ASS. Regarding the sulphur content of the co-substrates fed to the CSTR, most is fixed in the sludge by addition of FeCl and the H2S concentration of the CSTR biogas is very low. Only a smaller part of the total sulphur remains in the reject water recirculated to the water train of the plant.

- ECSB bypass can be allowed for 24h without exceeding plant discharge limits for NH_4-N and COD while P are exceeded during one day directly linked to each by-pass. Further simulations will be performed with aim to prevent the P-spikes and to reduce the COD and NH_4-N release at longer by-passes that is possibly needed linked to high levels of suspended matter in the primary effluent.
- The simulations of by-passing the ECSB showed that the plan to keep selector 3 semi-active as a sort of active sludge buffer, kicking in at increased COD-loads to the ASS linked to the by-passes likely will not work as planed but instead result in P-spikes. Further simulations are needed to study how a revised by-pass strategy should be taken in operation
- Shortening the sludge age in the ASS from 17 to 8 days will increase the amount of BOD5 and slowly biodegradable organics of the WAS which will likely have a positive effect on its biomethane potential.

6 Future research needs

- Investigate methane formation and oxidation in ASS both as standalone treatment and if in series with water train AD processes such as ECSB or IC.
- Impact of external substrate addition to ECSB. Glycerol is an interesting candidate and the effect of the sulphate concentration of the glycerol on both the gas production and on the fate of the increased amounts of reduced sulphured species in the ASS would be of interest to simulate using the model.
- Full-scale tests are needed to confirm the simulated dynamic response in ECSB and ASS from by-pass events. Future tests and simulations should be designed to evaluate the optimal operational strategy for the ASS during by-pass of the ECSB.
- Develop the model to be able to predict the fate of N, P, K and Ca in the dewatering i.e. how much will and up in the reject as dissolved salts and how much in the accept with the TSS.
- Yields of OHOs resulting from calibration of the model is lower than default values (0.5 compared to 0.67). Future studies should measure the yield, preferably at several plants for comparison.
- Time varying feed composition of co-substrates to CSTR. Pushing the limits of nutrient mineralization.
- Including more advanced AD-model for evaluating digester performance and stability, e.g. ADM1.
- Including more advanced model for ECSB-reactor for evaluating biomass growth, behaviour and reactor stability, e.g. three-phase model.
- Additional case studies at one or more plants.

References

Arnell, M., Astals, S., Åmand, L., Batstone, D.J., Jensen, P.D. and Jeppsson, U. 2016. Modelling anaerobic co-digestion in Benchmark Simulation Model No. 2: Parameter estimation, substrate characterisation and plant-wide integration. Water Research 98(C), 138-146.

Baeten, J.E., Batstone, D.J., Schraa, O.J., van Loosdrecht, M.C.M. and Volcke, E.I.P. 2019. Modelling anaerobic, aerobic and partial nitritation-anammox granular sludge reactors - A review. Water Research 149, 322-341.

Barat, R., Serralta, J., Ruano, M., Jiménez, E., Ribes, J., Seco, A. and Ferrer, J. 2013. Biological Nutrient Removal Model No. 2 (BNRM2): a general model for wastewater treatment plants. Water Science and Technology 67(7), 1481-1489.

Barker, P. and Dold, P. 1997. General model for biological nutrient removal activated-sludge systems: Model presentation. Water Environment Research 69(5), 969.

Batstone, D.J., Hülsen, T., Mehta, C.M. and Keller, J. 2015. Platforms for energy and nutrient recovery from domestic wastewater: A review. Chemosphere 140, 2-11.

Batstone, D.J., Keller, J., Angelidaki, I., Kalyuzhnyi, S.V., Pavalostathis, S.G., Rozzi, A., Sanders, W.T.M., Siegrist, H. and Vavilin, V.A. 2002. The IWA Anaerobic Digestion Model No 1 (ADM1). Water Science and Technology 45(10), 65-73.

Batstone, D.J., Tait, S. and Starrenburg, D. 2009. Estimation of hydrolysis parameters in full-scale anerobic digesters. Biotechnology and Bioengineering 102(5), 1513-1520.

Bolle, W.L., Van Breugel, J., Van Eybergen, G.C., Kossen, N.W.F. and Van Gils, W. 1986. An integral dynamic model for the UASB reactor. Biotechnology and Bioengineering 28(11), 1621-1636.

Brault, J.-M., Comeau, Y., Perrier, M. and Stuart, P. 2010. Modeling Thermomechanical Pulp and Paper Activated Sludge Treatment Plants to Gain Insight to the Causes of Bulking. Water Environment Research 82(4), 362-373.

Costello, D.J., Greenfield, P.F. and Lee, P.L. 1991. Dynamic modelling of a single-stage high-rate anaerobic reactor—II. Model verification. Water Research 25(7), 859-871.

Diamantis, V. and Aivasidis, A. 2018. Performance of an ECSB reactor for high-rate anaerobic treatment of cheese industry wastewater: effect of pre-acidification on process efficiency and calcium precipitation. Water Science and Technology 78(9), 1893-1900.

Eddy, M., Burton, F., Tchobanoglous, G. and Tsuchihashi, R. 2013 Wastewater engineering: treatment and resource recovery, McGraw-Hill Education: New York, NY, USA.

Fuentes, M., Scenna, N.J. and Aguirre, P.A. 2011. A coupling model for EGSB bioreactors: Hydrodynamics and anaerobic digestion processes. Chemical Engineering and Processing: Process Intensification 50(3), 316-324.

Ge, H., Batstone, D.J. and Keller, J. 2013. Operating aerobic wastewater treatment at very short sludge ages enables treatment and energy recovery through anaerobic sludge digestion. Water Research 47(17), 6546-6557.

Ge, H., Batstone, D.J., Mouiche, M., Hu, S. and Keller, J. 2017. Nutrient removal and energy recovery from high-rate activated sludge processes – Impact of sludge age. Bioresource Technology 245, 1155-1161.

Gernaey, K.V., van Loosdrecht, M.C.M., Henze, M., Lind, M. and Jørgensen, S.B. 2004. Activated sludge wastewater treatment plant modelling and simulation: state of the art. Environmental Modelling and Software 19(9), 763-783.

Gernaey, K.V., Jeppsson, U., Vanrolleghem, P.A. and Copp, J. B. 2014 Benchmarking of control strategies for wastewater treatment plants. IWA Scientific and Technical Report No. 21, London : IWA Publ.

Hauduc, H., Wadhawan, T., Johnson, B., Bott, C., Ward, M. and Takács, I. 2018. Incorporating sulfur reactions and interactions with iron and phosphorus into a general plant-wide model. Water Science and Technology 79(1), 26-34.

Henze, M. 2000 Activated sludge models ASM1, ASM2, ASM2d and ASM3, London : IWA Publ.

Henze, M., van Loosdrecht, M.C.M., Ekama, G.A. and Brdjanovic, D. 2008 Biological Wastewater Treatment – Principles, Modelling and Design. London, U.K. : IWA Publ.

Horan, N. and Chen, W. 1998. The treatment of a high strength pulp and paper mill effluent for waste water re-use: I, the use of modelling to optimise effluent quality from the existing wastewater treatment plant. Environmental Technology 19(2), 153-161.
Jensen, P.D., Ge, H. and Batstone, D.J. 2011. Assessing the role of biochemical methane potential tests in determining anaerobic degradability rate and extent. Water Sci. Technol. 64(4), 880-886.
Jeppsson, U., Nopens, I., Alex, J., Copp, J., Gernaey, K., Rosen, C. and Vanrolleghem, P. 2007. Benchmark simulation model no 2: general protocol and exploratory case studies. Water Science and Technology 56(8), 67-78.
Jimenez, J., Miller, M., Bott, C., Murthy, S., De Clippeleir, H. and Wett, B. 2015. High-rate activated sludge system for carbon management – Evaluation of crucial process mechanisms and design parameters. Water Research 87(C), 476-482.
Jimenez, J.A., La Motta, E.J. and Parker, D.S. 2005. Kinetics of Removal of Particulate Chemical Oxygen Demand in the Activated-Sludge Process. Water Environment Research 77(5), 437-446.
Kazadi Mbamba, C., Batstone, D.J., Flores-Alsina, X. and Tait, S. 2015. A generalised chemical precipitation modelling approach in wastewater treatment applied to calcite. Water Research 68, 342-353.
Lindblom, E., Rosen, C., Vanrolleghem, P., Olsson, L.E. and Jeppsson, U. 2004 Modelling a nutrient deficient wastewater treatment process.
Magnusson, B., Ekstrand, E.-M., Karlsson, A. and Ejlertsson, J. 2018. Combining high-rate aerobic wastewater treatment with anaerobic digestion of waste activated sludge at a pulp and paper mill. Water science and technology : a journal of the International Association on Water Pollution Research 77(7-8), 2068.
Melcer, H. (2003) Methods for wastewater characterization in activated sludge modeling, Alexandria, VA : Water Environment Federation and London, U.K. : IWA Pub.
Meyer, T. and Edwards, E.A. 2014. Anaerobic digestion of pulp and paper mill wastewater and sludge. Water Research 65(C), 321-349.
Nopens, I., Batstone, D.J., Copp, J.B., Jeppsson, U., Volcke, E., Alex, J. and Vanrolleghem, P.A. 2009. An ASM/ADM model interface for dynamic plant-wide simulation. Water Research 43(7), 1913-1923.
Pokhrel, D. and Viraraghavan, T. 2004. Treatment of pulp and paper mill wastewater—a review. Science of the Total Environment 333(1), 37-58.
Richardson, D.A., Andras, E. and Kennedy, K.J. 1991. Anaerobic Toxicity of Fines in Chemi-Thermomechanical Pulp Wastewaters: A Batch Assay-Reactor Study Comparison. Water Science and Technology 24(3-4), 103-112.
Seco, A., Ribes, J., Serralta, J. and Ferrer, J. 2004. Biological nutrient removal model No. 1 (BNRM1). Water Science and Technology 50(6), 69-70.
Stoica, A., Sandberg, M. and Holby, O. 2009. Energy use and recovery strategies within wastewater treatment and sludge handling at pulp and paper mills. Bioresource Technology 100(14), 3497-3505.
Varga, E., Hauduc, H., Barnard, J., Dunlap, P., Jimenez, J., Menniti, A., Schauer, P., Lopez Vazquez, C.M., Gu, A.Z., Sperandio, M. and Takács, I. 2018. Recent advances in bio-P modelling – a new approach verified by full-scale observations. Water Science and Technology 78(10), 2119-2130.
Veluchamy, C. and Kalamdhad, A.S. 2017. Influence of pretreatment techniques on anaerobic digestion of pulp and paper mill sludge: A review. Bioresource Technology 245(PA), 1206-1219.

Through our international collaboration programmes with academia, industry, and the public sector, we ensure the competitiveness of the Swedish business community on an international level and contribute to a sustainable society. Our 2,800 employees support and promote all manner of innovative processes, and our roughly 100 testbeds and demonstration facilities are instrumental in developing the future-proofing of products, technologies, and services. RISE Research Institutes of Sweden is fully owned by the Swedish state.

I internationell samverkan med akademi, näringsliv och offentlig sektor bidrar vi till ett konkurrenskraftigt näringsliv och ett hållbart samhälle. RISE 2 800 medarbetare driver och stöder alla typer av innovationsprocesser. Vi erbjuder ett 100-tal test- och demonstrationsmiljöer för framtidssäkra produkter, tekniker och tjänster. RISE Research Institutes of Sweden ägs av svenska staten.

RISE Research Institutes of Sweden AB
Gjuterigatan 1D, SE-582 73 LINKÖPING, Sweden
Telephone: +46 10 516 50 00
E-mail: info@ri.se, Internet: www.ri.se

System Transition and
Service Innovation
RISE Report 2020:53
ISBN: 978-91-89167-36-0